

## SUPPORTING INFORMATION

### Configurationally stable dithia[7]helicene and dithia-quasi[8]circulene fused dithiolones

Maxime Baudillon,<sup>a</sup> Thomas Cauchy,<sup>a</sup> Nicolas Vanthuynne,<sup>b</sup> Narcis Avarvari<sup>\*,a</sup> and Flavia Pop<sup>\*,a</sup>

<sup>a</sup> Univ Angers, CNRS, MOLTECH-Anjou, SFR MATRIX, F-49000 Angers, France.

<sup>b</sup> Aix Marseille Université, CNRS, Centrale Marseille, iSm2, Marseille, France.

### Table of contents

<b>1. General methods and materials</b> .....	2
<b>2. Syntheses and NMR characterization</b> .....	2
2.1. Synthesis of 1,2-bis(naphtho[2,1-b]thiophen-2-yl)ethyne (3).....	2
2.2. Synthesis of 4,5-bis(naphtho[2,1-b]thiophen-2-yl)-1,3-dithiol-2-one (4).....	4
2.3. Synthesis of naphtho[1'',2'':4',5']thieno[2',3':3,4]naphtho[1'',2'':4',5']thieno[3',2':5,6]benzo[1,2- d][1,3]dithiol-9-one (1-dTH) .....	6
2.4. Synthesis of 1-dTQC .....	7
2.5. Synthesis of 1-dTQC -Cl .....	9
<b>3. Single crystal X-ray diffraction</b> .....	11
<b>4. Racemisation barrier and enantiomer resolution</b> .....	18
4.1. Chiral HPLC.....	18
4.2. Optical rotations .....	21
4.3. Kinetic of enantiomerisation .....	22
1-dTH in 1,2-dichlorobenzene .....	22
1-dTQC in chlorobenzene .....	23
<b>5. Absorption and circular dichroism properties</b> .....	24
<b>6. Theoretical calculations</b> .....	25
6.1. Computational details .....	25
6.2. Results.....	26

## 1. General methods and materials

All commercially available reagents and solvents were used as received unless otherwise noted. Dry diethyl ether was directly used from the purification machines. Chloroform and tetrahydrofuran as solvents for synthesis and extraction were used as supplied. Naphtho[2,1-b]-thiophene<sup>1</sup> and 2-bromonaphtho[2,1-b]-thiophene **2**<sup>2</sup> were synthesized according to previously reported procedures. Chromatography purifications were performed on silica gel Sorbent Technologies Silica Gel (60 Å, 65 x 250 mesh) and thin layer chromatography (TLC) was carried out using aluminum sheets precoated with silica gel 60 (EMD 40–60 mm, 230–400 mesh with 254 nm dye). NMR spectra were acquired on a Bruker Avance DRX 300 and 500 spectrometers operating at 300 and 500 MHz for <sup>1</sup>H and 75 and 125 MHz for <sup>13</sup>C, respectively, at room temperature in CDCl<sub>3</sub> solutions. <sup>1</sup>H and <sup>13</sup>C NMR spectra were referenced to the residual protonated solvent (<sup>1</sup>H) or the solvent itself (<sup>13</sup>C). All chemical shifts are expressed in parts per million (ppm) downfield from external tetramethylsilane (TMS), using the solvent residual signal as an internal standard and the coupling constant values (J) are reported in Hertz (Hz). The following abbreviations have been used: s, singlet; d, doublet; t, triplet; q, quadruplet; dd, doublet of doublets; td, triplet of doublets; m, multiplet. Mass spectrometry MALDI–TOF MS and HRMS analyses were recorded on JEOL JMS3000 (MALDI/TOF-TOF) spectrometer. In all cases the used matrix was DCTB trans-2-[3-(4-t-butyl-phenyl)-2-methyl-2-propenylidene]malononitrile. Elemental analyses were recorded using Flash 2000 Fisher Scientific Thermo Electron analyser. UV-Vis-NIR absorption spectra were recorded using a Perkin Elmer L950 spectrometer in CH<sub>2</sub>Cl<sub>2</sub> solutions. Electrochemical experiments were performed with a SP150 Biologic Potentiostat in a standard three-electrode cell using platinum working disk electrodes of 2 mm diameter and 0.1 M TBAPF<sub>6</sub> in dichloromethane as supporting electrolyte, with scan rates between 50 and 500 mV/s. Ferrocene has been used as internal reference and values reported versus standard calomel electrode (SCE). Details about data collection and solution refinement are given in Tables S2 and S3. Single crystals of the compounds were mounted on glass fibre loops using a viscous hydrocarbon oil to coat the crystal and then transferred directly to cold nitrogen stream for data collection. X-ray single-crystal diffraction data were collected at 150K and 230 K on an Agilent SuperNova diffractometer equipped with Atlas CCD detector and mirror monochromated micro-focus Cu-K<sub>α</sub> radiation ( $\lambda = 1.54184 \text{ \AA}$ ). The structure was solved by direct methods, expanded and refined on F<sup>2</sup> by full matrix least-squares techniques using SHELX programs (G.M. Sheldrick, 2016). All non-H atoms were refined anisotropically and the H atoms were included in the calculation without refinement. Multi-scan empirical absorption was corrected using CrysAlisPro program (CrysAlisPro, Agilent Technologies, V1.171.37.35g, 2014). Crystallographic data of the structures obtained at 150 K have been deposited with the Cambridge Crystallographic Data Centre, deposition numbers CCDC 2160878 (**2**), CCDC 2160879 (**4**), CCDC 2160880 (*(rac)*-**1-dTH**) and CCDC 2160881 (*(rac)*-**1-dTQC**). These data can be obtained free of charge from CCDC, 12 Union road, Cambridge CB2 1EZ, UK (e-mail: deposit@ccdc.cam.ac.uk or <http://www.ccdc.cam.ac.uk>).

## 2. Syntheses and NMR characterization

### 2.1. Synthesis of 1,2-bis(naphtho[2,1-b]thiophen-2-yl)ethyne (**3**)

Compound **2a** (1.3 g, 5 mmol), calcium carbide (1.6 g, 25 mmol), copper iodide (I) (0.048 g, 0.25 mmol), triethylamine (1.4 ml, 10 mmols), tetrakis(triphenylphosphine)palladium(0) (0.14 g, 0.125 mmol) were added to a two neck reaction tube followed by dimethylformamide (8 ml). The reaction tube was closed with a septum and a balloon to collect the acetylene gas. Water (0.54 ml, 30 mmol) was added dropwise with a syringe to release the acetylene gas. The reaction mixture was further stirred at 65°C for 24 hours. Water was added and the solid was filtered and further washed with water and dichloromethane. The remaining solid was extracted in a Soxhlet apparatus with chloroform followed by a mixture of chloroform/tetrahydrofuran 1/1. The dichloromethane filtrate was purified by column chromatography (silica gel, petroleum ether/dichloromethane 4/1) to afford 200 mg of impure product and its purity could not be further improved. The two solid-liquid extractions at high temperature afforded the desired product as pale yellow solid of high purity (312 mg, yield 32%).

Quantitative yields have been obtained for the synthesis of 1,2-bis(naphtho[2,1-b]thiophen-2-yl)ethyne (**3**) when 2-iodonaphtho[2,1-b]-thiophene **2b** has been used instead of 2-bromonaphtho[2,1-b]-thiophene (**2a**).

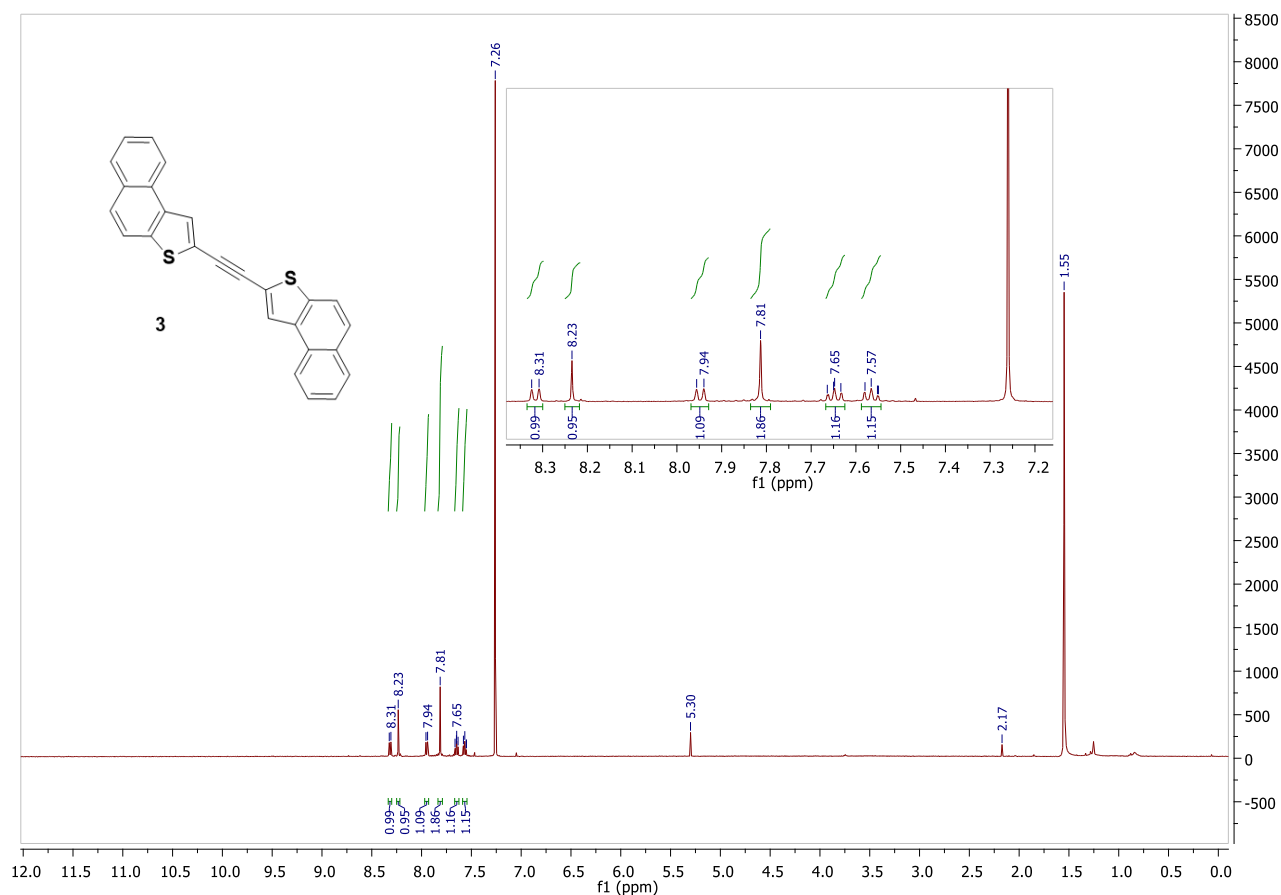
$^1\text{H}$  NMR (500 MHz,  $\text{CDCl}_3$ )  $\delta$  8.32 (d,  $J = 8.3$  Hz, 1H), 8.23 (s, 1H), 7.95 (d,  $J = 8.1$  Hz, 1H), 7.81 (m, 2H), 7.65 (dd,  $J = 6.8$  Hz, 1H), 7.57 (dd,  $J = 6.9$  Hz, 1H).

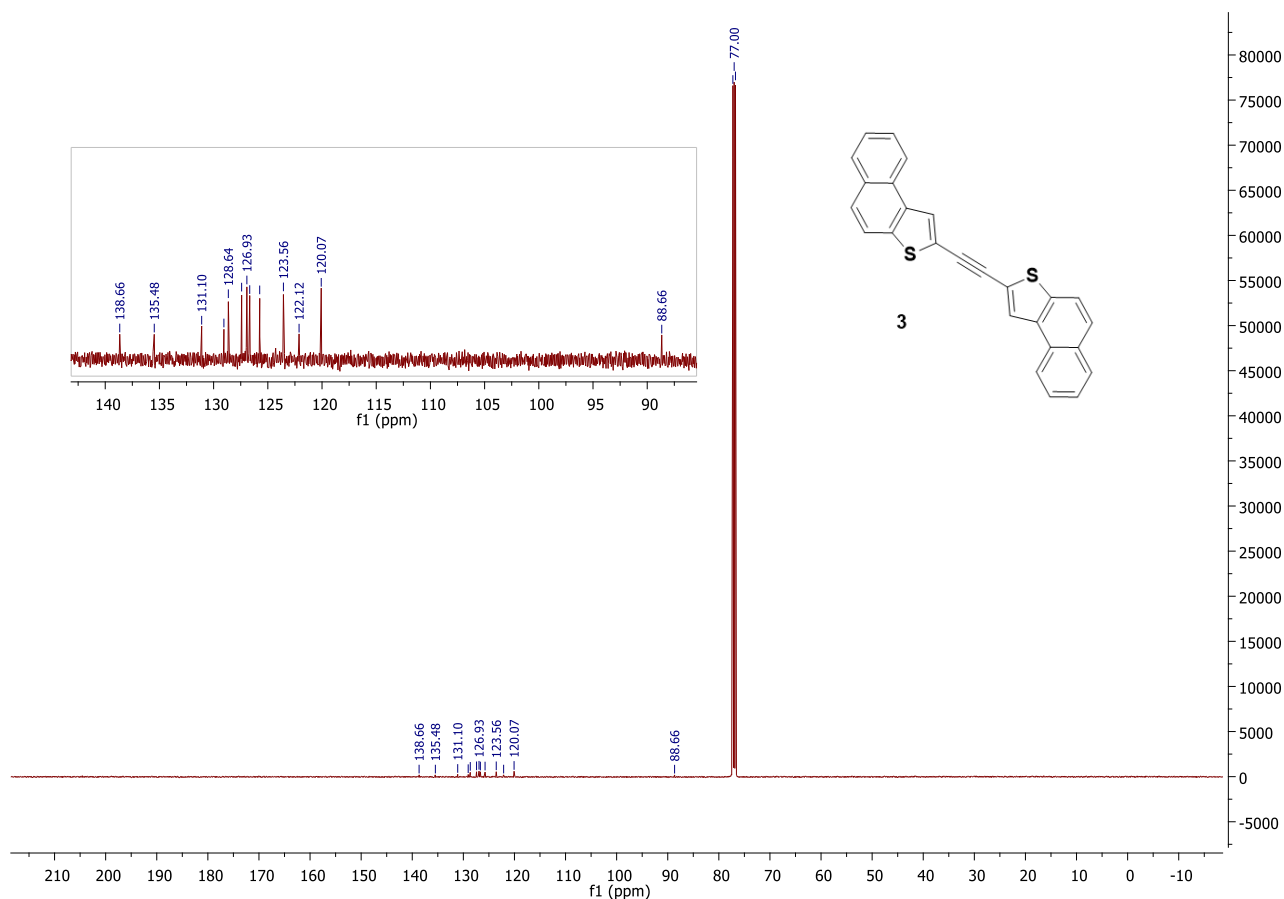
$^{13}\text{C}$  NMR (126 MHz,  $\text{CDCl}_3$ )  $\delta$  138.6, 135.5, 131.1, 129.0, 128.6, 127.4, 126.9, 126.6, 125.7, 123.5, 122.1, 120.0, 88.6.

Elemental analysis calcd. (%) for  $\text{C}_{26}\text{H}_{14}\text{S}_2$ : C 79.96, H 3.61, S 16.42; found: C 77.61, H 3.56, S 15.26.

HRMS (TOF) calcd for  $\text{C}_{26}\text{H}_{14}\text{S}_2$   $[\text{M}^+]$ : 390.05314, found 390.05348 (error 0.85 ppm).

MS (MALDI-TOF) Mth = 390.05; observed  $m/z = 390.0$ .





## 2.2. Synthesis of 4,5-bis(naphtho[2,1-b]thiophen-2-yl)-1,3-dithiol-2-one (4)

Compound **3** (300 mg, 0.77 mmol) and diisopropyl xanthogen disulphide (208 mg, 0.77 mmol) were dissolved in deoxygenated chlorobenzene (15 mL). AIBN (63 mg, 0.385 mmol) was added and the reaction mixture was stirred at 90°C for 20 hours. The solid (100 mg of unreacted starting material) was filtered and the filtrate was concentrated and purified by column chromatography (silica gel, petroleum ether/dichloromethane 7/3). The desired product was isolated as orange powder (200 mg, yield 53%) Conversion of the starting material 66%, yield based on converted material 81%.

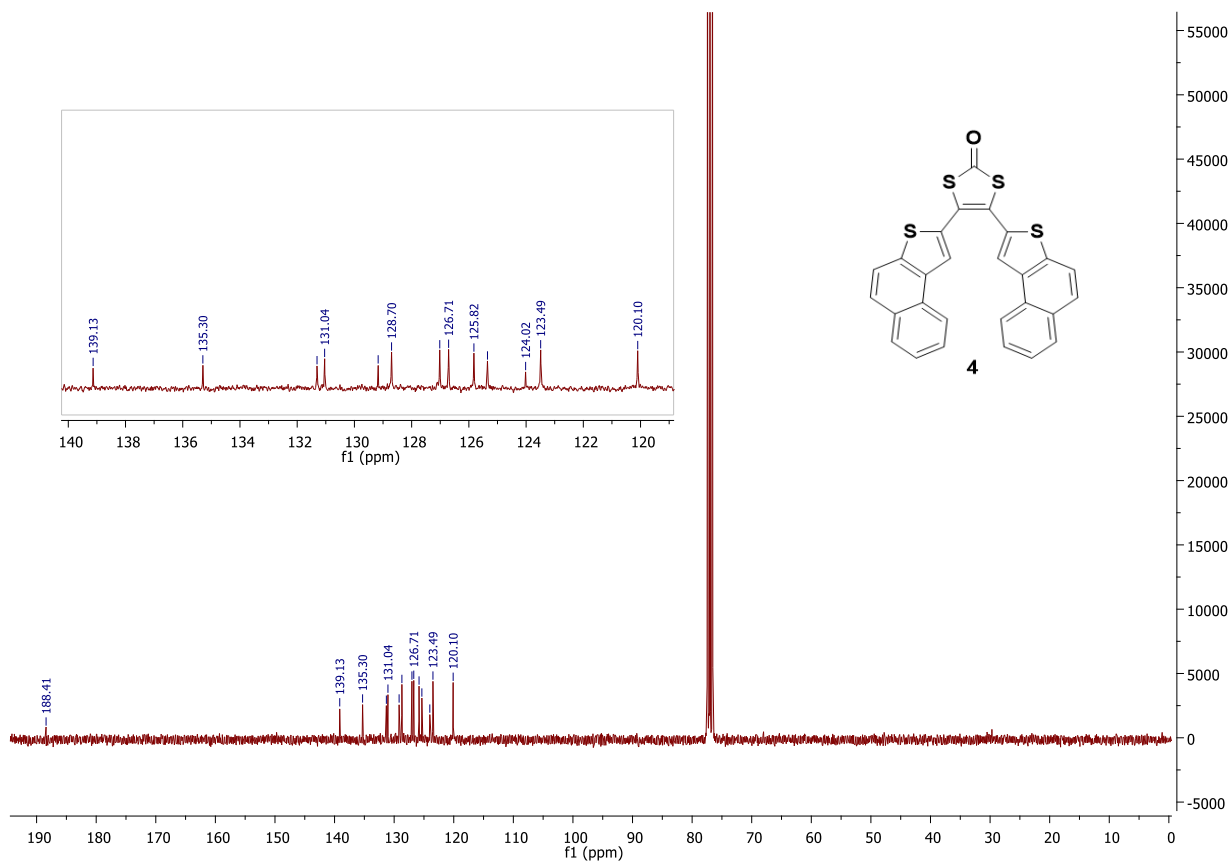
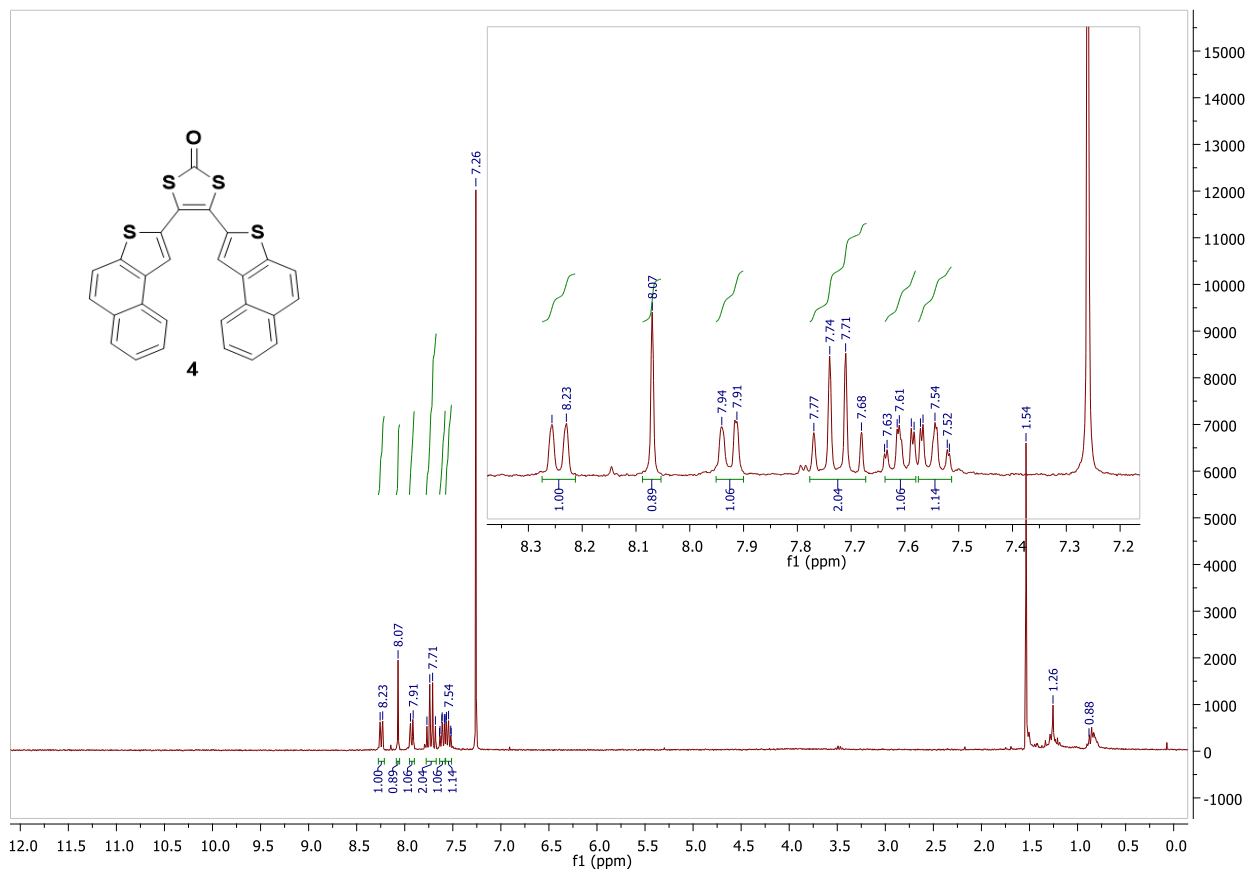
$^1\text{H}$  NMR (300 MHz,  $\text{CDCl}_3$ )  $\delta$  8.24 (d,  $J = 8.0$  Hz, 1H), 8.06 (s, 1H), 7.92 (d,  $J = 7.5$  Hz, 1H), 7.72 (dd,  $J = 8.8$  Hz, 2H), 7.64 – 7.58 (m, 1H), 7.57 – 7.51 (m, 1H).

$^{13}\text{C}$  NMR (76 MHz,  $\text{CDCl}_3$ )  $\delta$  188.4, 139.1, 135.3, 131.3, 131.0, 129.1, 128.7, 127.0, 126.7, 125.8, 125.3, 124.0, 123.4, 120.1.

Elemental analysis calcd. (%) for  $\text{C}_{27}\text{H}_{14}\text{O}_4\text{S}_4$ : C 67.19, H 2.92, O 3.31, S 26.57; found: C 66.11, H 2.92, S 25.61.

HRMS (TOF) calcd for  $\text{C}_{27}\text{H}_{14}\text{O}_4\text{S}_4$  [ $\text{M}^+$ ]: 481.99301, found 481.99220 (error 1.69 ppm).

MS (MALDI-TOF)  $m/z$  = 481.99; observed  $m/z$  = 481.9.



### 2.3. Synthesis of

#### naphtho[1'',2'':4',5']thieno[2',3':3,4]naphtho[1'',2'':4',5']thieno[3',2':5,6]benzo[1,2-d][1,3]dithiol-9-one (1-dTH)

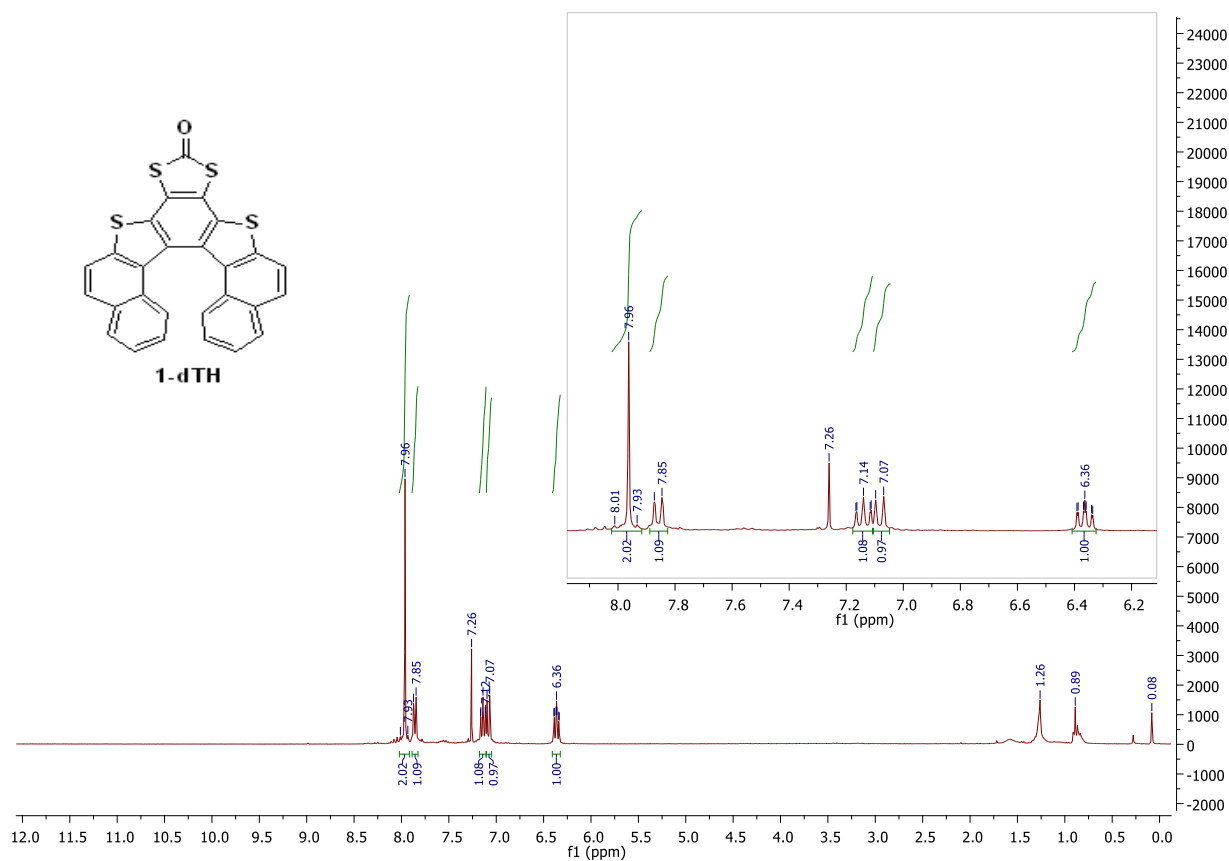
Compound **4** (200 mg, 0.414 mmol) was dissolved in dry dichloromethane (10 mL) and cooled at  $-78^{\circ}\text{C}$ . Phenyliodine bis(trifluoroacetate) (PIFA) (214 mg, 0.5 mmol) and boron trifluoride diethyl etherate ( $\text{BF}_3\cdot\text{Et}_2\text{O}$ ) (0.12 mL, 1 mmol) were added as solution in 5 ml of dichloromethane, and the reaction was stirred for 1 hour at  $-78^{\circ}\text{C}$  then allowed to reach room temperature. The reaction was quenched with water and extracted with dichloromethane. The crude was purified by column chromatography (silica gel, petroleum ether/dichloromethane 7/3) to afford some unreacted starting material and the desired product as a yellow powder (91 mg, yield 45%).

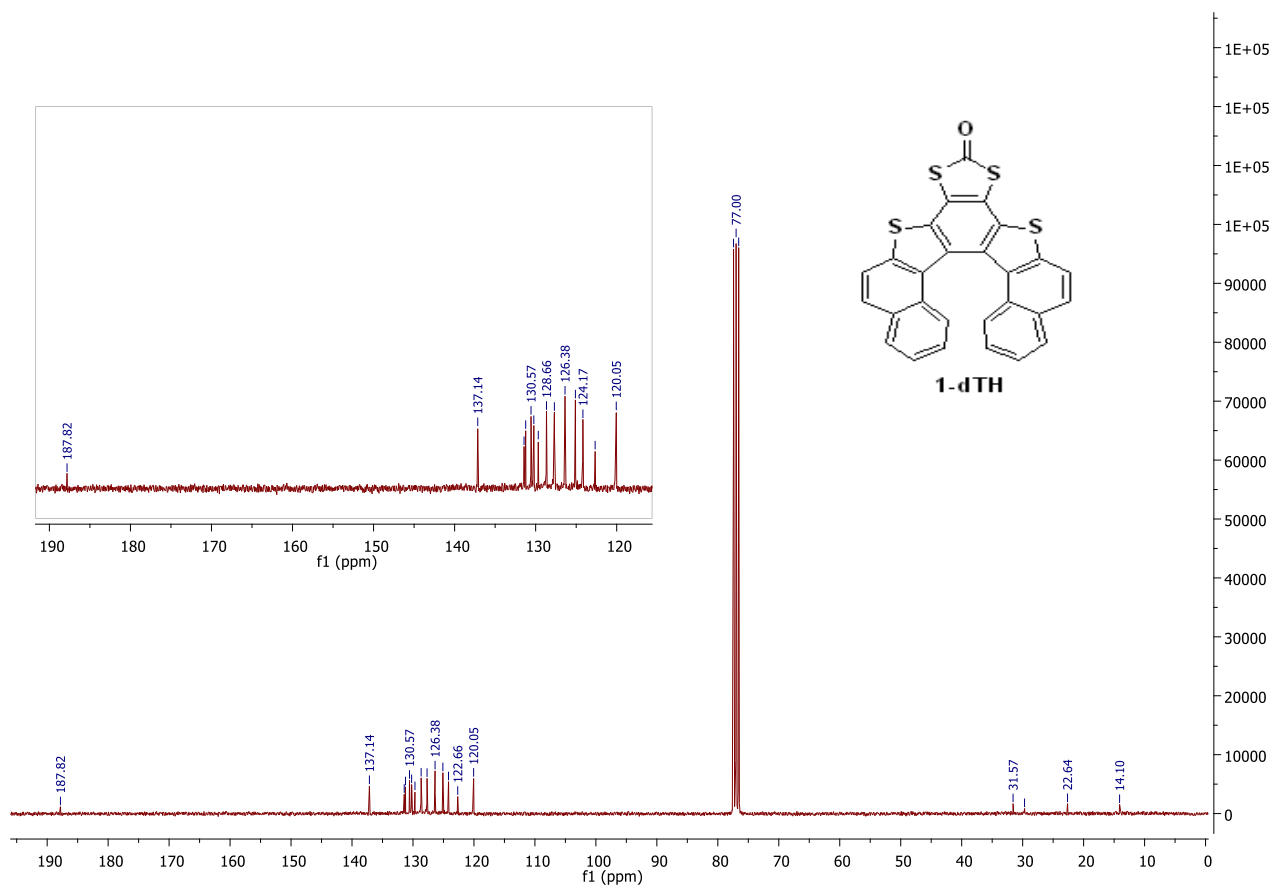
$^1\text{H}$  NMR (300 MHz,  $\text{CDCl}_3$ )  $\delta$  8.02 – 7.92 (m, 2H), 7.86 (d,  $J = 8.1$  Hz, 1H), 7.18 – 7.11 (m, 1H), 7.08 (d,  $J = 8.4$  Hz, 1H), 6.36 (ddd,  $J = 8.3, 6.9, 1.2$  Hz, 1H).

$^{13}\text{C}$  NMR (76 MHz,  $\text{CDCl}_3$ )  $\delta$  187.8, 137.1, 131.4, 131.2, 130.5, 130.2, 129.7, 128.7, 127.7, 126.4, 125.1, 124.2, 122.7, 120.1.

HRMS (TOF) calcd for  $\text{C}_{27}\text{H}_{12}\text{OS}_4$  [ $\text{M}^+$ ]: 479.97655, found 479.97780 (error 2.6 ppm).

MS (MALDI-TOF)  $M_{\text{th}} = 479.98$ ; observed  $m/z = 480.0$ .





## 2.4. Synthesis of 1-dTQC

Method 1. Compound **4** (3 mg, 6.2  $\mu\text{mol}$ ) was dissolved in chloroform (0.5 mL).  $\text{FeCl}_3$  (10 mg, 62  $\mu\text{mol}$ ) was added as solution in nitromethane (0.5 mL). The reaction was stirred for 1 hour and stopped by quenching with methanol. The solution was concentrated and the crude was purified by filtration on silica using dichloromethane to remove the excess of  $\text{FeCl}_3$ , followed by column chromatography (silica gel, petroleum ether/dichloromethane 7/3) to afford a yellow powder. With 1 eq. of  $\text{FeCl}_3$  was used a mixture of unreacted starting material, helicene and the desired circulene has been obtained whereas when up to 1 eq. of  $\text{FeCl}_3$  were used the desired **1-dTQC** has been obtained quantitatively (Table 1).

Method 2. Compound **4** (10 mg, 0.02 mmol) was dissolved in dry dichloromethane (4 mL) and cooled at  $-78^\circ\text{C}$ . PIFA (13.4 mg, 0.025 mmol) and  $\text{BF}_3 \cdot \text{Et}_2\text{O}$  (5.6 mL, 45 mmol) were added and the solution was stirred for 30 minutes at  $-78^\circ\text{C}$ . The reaction was quenched with water and extracted with dichloromethane. The crude was purified by column chromatography (silica gel, petroleum ether/dichloromethane 7/3) to afford a yellow powder in quantitative yields.

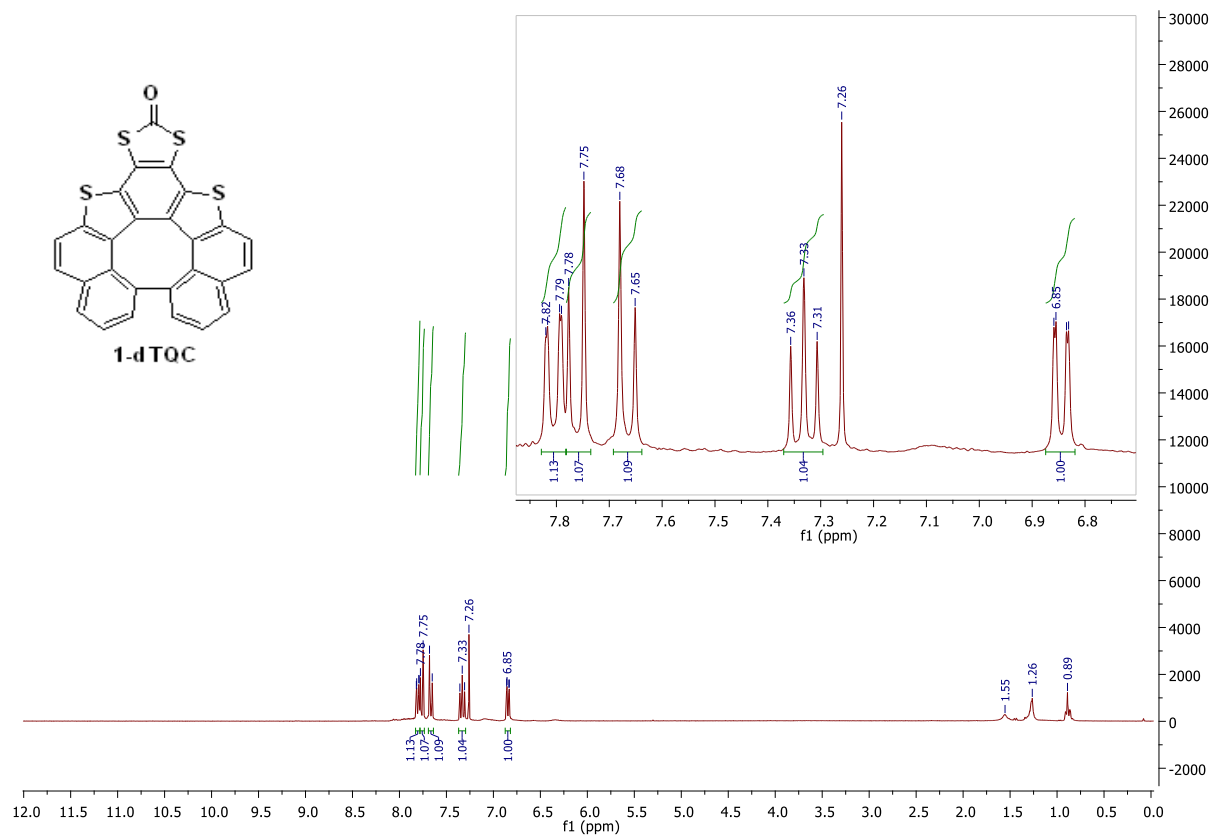
Method 3. **1-dTH** (4 mg, 8.3  $\mu\text{mol}$ ) was dissolved in toluene 3 ml. 2,3-dichloro-5,6-dicyano-1,4-benzoquinone (DDQ) (20 mg, 41.6  $\mu\text{mol}$ ) and scandium triflate (9 mg, 41.6  $\mu\text{mol}$ ) were added under argon. The mixture was stirred for 24 h at room temperature and 20 h at  $110^\circ\text{C}$ . The mass analysis of two samples room temperature and  $110^\circ\text{C}$  show the formation of the desired product in both cases together with unreacted starting material. The mixture was separated by column chromatography (silica gel, petroleum ether/dichloromethane 7/3) to afford a yellow powder (2.4 mg, yield 60%).

<sup>1</sup>H NMR (300 MHz,  $\text{CDCl}_3$ )  $\delta$  7.81 (dd,  $J = 7.9, 1.1$  Hz, 1H), 7.76 (d,  $J = 8.6$  Hz, 1H), 7.67 (d,  $J = 8.7$  Hz, 1H), 7.33 (t,  $J = 7.5$  Hz, 1H), 6.85 (dd,  $J = 7.2, 1.2$  Hz, 1H).

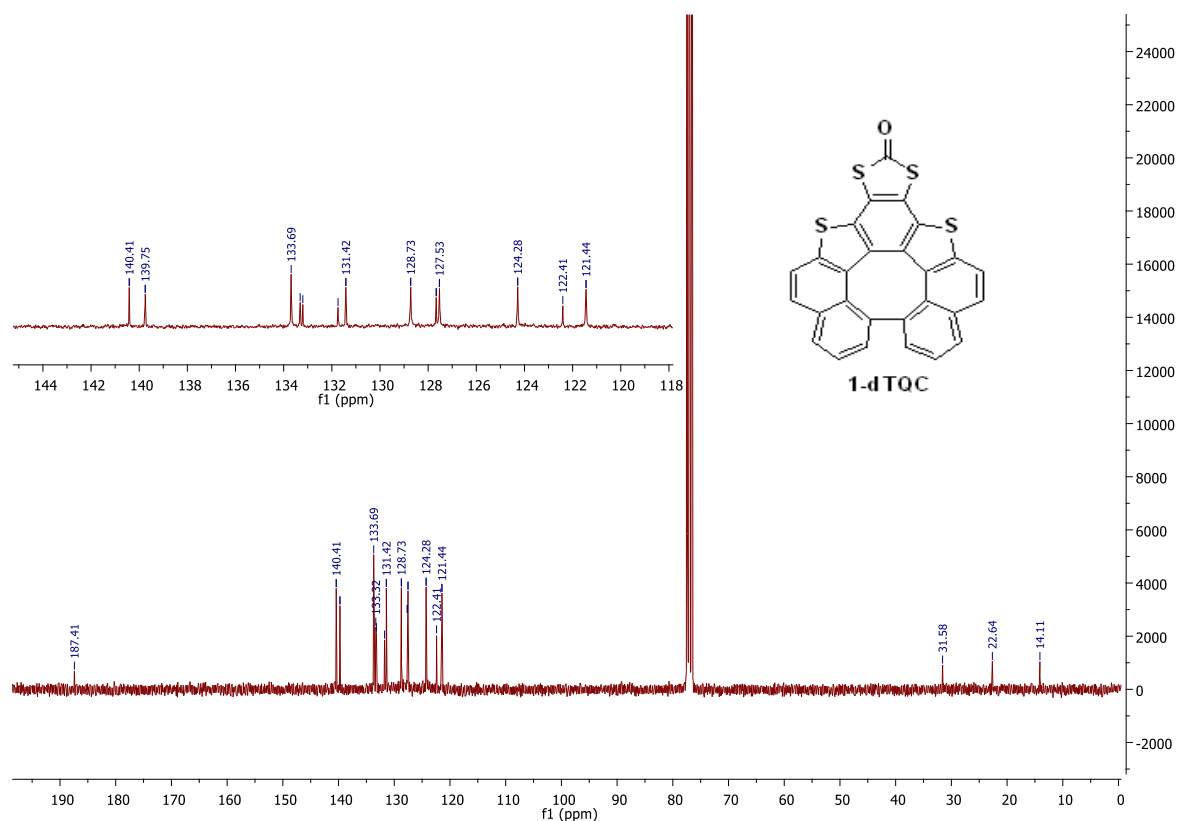
$^{13}\text{C}$  NMR (126 MHz,  $\text{CDCl}_3$ )  $\delta$  187.4, 140.4, 139.8, 133.7, 133.3, 133.2, 131.7, 131.4, 128.7, 127.7, 127.5, 124.3, 122.4, 121.4.

HRMS (TOF) calcd for  $\text{C}_{27}\text{H}_{10}\text{OS}_4$   $[\text{M}^+]$ : 477.96090, found 477.96196 (error 2.22 ppm).

MS (MALDI-TOF) Mth = 477.96; observed  $m/z$  = 478.0.







## 2.5. Synthesis of 1-dTQC -Cl

Compound **4** (1 mg, 2  $\mu\text{mol}$ ) and  $\text{FeCl}_3$  (large excess) were dissolved in chloroform and stirred at room temperature during the week-end. The solution filtered through silica gel using dichloromethane to remove the excess of  $\text{FeCl}_3$ . The solution was then concentrated and recrystallized from a mixture of dichloromethane and diethyl ether to afford the desired product in quantitative yields.

$^1\text{H}$  NMR (300 MHz,  $\text{CDCl}_3$ )  $\delta$  8.38 – 8.33 (m, 1H), 8.03 (s, 1H), 7.51 – 7.44 (m, 1H), 6.89 (d,  $J = 8.4$  Hz, 1H).

Due to small reaction scale and small amount of isolated compound,  $^{13}\text{C}$  NMR could not be performed. MS (MALDI-TOF)  $M_{\text{th}} = 545.88$ ; observed  $m/z = 517.8$  (M-CO).

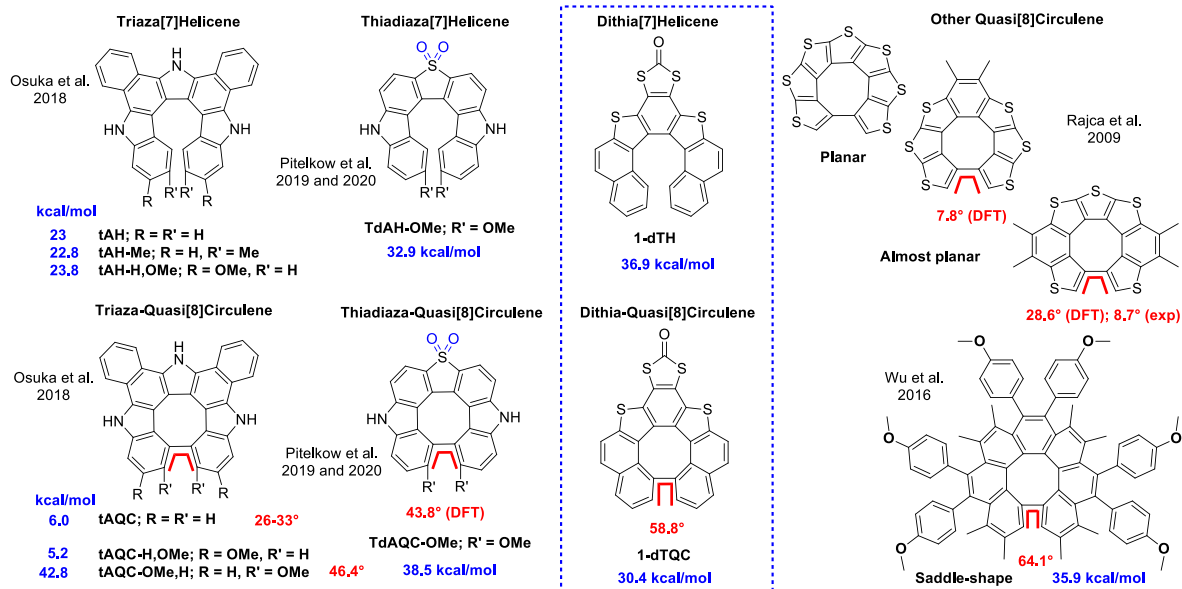
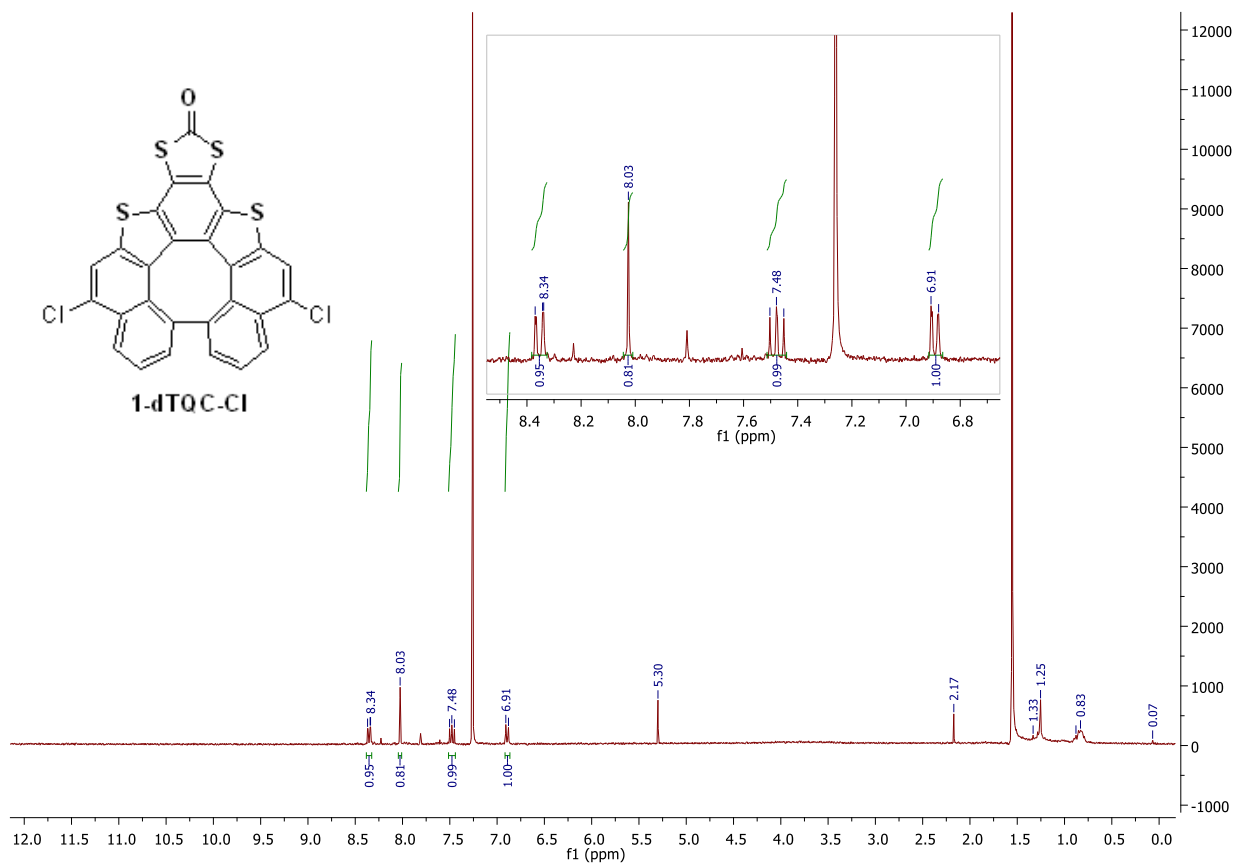


Figure S1. Hetero-[7]Helicenes et Quasi[8]Circulenes, previously described in the literature and those of this project (blue rectangle). Experimental and calculated torsion angles of the termini rings are highlighted in red, and calculated racemization barriers are highlighted in blue.

Table S1. Oxidative dehydrocyclisation conditions of dithia[7]helicene **1-dTH**.

	<b>Oxidant</b>	<b>Eq.</b>	<b>Solvent</b>	<b>Reaction time</b>	<b>Product</b>
<b>1</b>	Solid FeCl <sub>3</sub>	Excess	CHCl <sub>3</sub>	60 h ( <i>rt</i> )	<b>1-dTH</b>
<b>2</b>	Solution of FeCl <sub>3</sub> / CH <sub>3</sub> NO <sub>2</sub>	10	CHCl <sub>3</sub> / CH <sub>3</sub> NO <sub>2</sub>	1 hr ( <i>rt</i> )	<b>1-dTH</b>
<b>3</b>	Chloranil- BF <sub>3</sub> ·Et <sub>2</sub> O	1	CH <sub>2</sub> Cl <sub>2</sub>	45 min (0 °C)	<b>1-dTH</b>
<b>4</b>	DDQ-Sc(OTf) <sub>3</sub>	5	Toluene	12h ( <i>rt</i> ); 20h (reflux)	<b>1-dTH+1-dTQC</b>

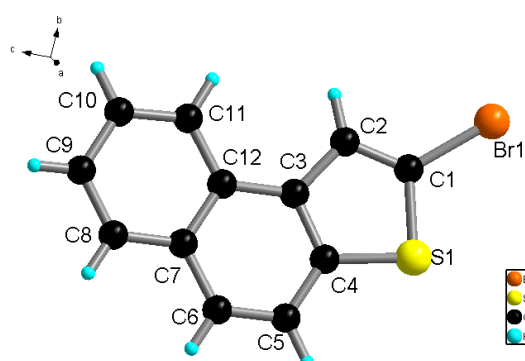
### 3. Single crystal X-ray diffraction

Table S2. Crystal data and structure refinement.

	<b>2</b>	<b>4</b>
Identification code	<b>2</b>	<b>4</b>
Empirical formula	C <sub>12</sub> H <sub>7</sub> BrS	C <sub>27</sub> H <sub>14</sub> OS <sub>4</sub>
Formula weight	263.15	482.62
Temperature/K	150.2(7)	150.0(1)
Crystal system	monoclinic	monoclinic
Space group	P2 <sub>1</sub> /c	P2 <sub>1</sub> /c
a/Å	7.5776(10)	18.2353(7)
b/Å	6.4074(8)	5.6303(2)
c/Å	20.676(2)	21.2483(10)
α/°	90	90
β/°	90.095(12)	105.297(4)
γ/°	90	90
Volume/Å <sup>3</sup>	1003.9(2)	2104.28(15)
Z	4	4
ρ <sub>calc</sub> /cm <sup>3</sup>	1.741	1.523
μ/mm <sup>-1</sup>	7.114	4.300
F(000)	520.0	992.0
Crystal size/mm <sup>3</sup>	0.092 × 0.045 × 0.023	0.259 × 0.096 × 0.058
Radiation	CuKα (λ = 1.54184)	CuKα (λ = 1.54184)
2θ range for data collection/°	8.554 to 145.192	5.024 to 152.088
Index ranges	-9 ≤ h ≤ 7, -6 ≤ k ≤ 7, -25 ≤ l ≤ 25	-22 ≤ h ≤ 22, -6 ≤ k ≤ 6, -23 ≤ l ≤ 26
Reflections collected	3635	8766
Independent reflections	1776 [R <sub>int</sub> = 0.0539, R <sub>sigma</sub> = 0.0667]	4268 [R(int) = 0.0166, R <sub>sigma</sub> = 0.0238]
Data/restraints/parameters	1776/0/127	4268 / 0 / 353
Goodness-of-fit on F <sup>2</sup>	1.136	1.031
Final R indexes [I >= 2σ (I)]	R <sub>1</sub> = 0.0831, wR <sub>2</sub> = 0.1824	R <sub>1</sub> = 0.0391, wR <sub>2</sub> = 0.1048
Final R indexes [all data]	R <sub>1</sub> = 0.0948, wR <sub>2</sub> = 0.1883	R <sub>1</sub> = 0.0459, wR <sub>2</sub> = 0.1112
Largest diff. peak/hole / e Å <sup>-3</sup>	1.14/-0.90	0.268/-0.400

Table S3. Crystal data and structure refinement.

Identification code	<b>1-dTH (<i>rac</i>)</b>	<b>1-dTQC (<i>rac</i>)</b>	<b>1-dTQC-Cl (<i>rac</i>)</b>
Empirical formula	C <sub>54</sub> H <sub>24</sub> O <sub>2</sub> S <sub>8</sub>	C <sub>27</sub> H <sub>10</sub> OS <sub>4</sub>	C <sub>27</sub> H <sub>8</sub> Cl <sub>2</sub> OS <sub>4</sub>
Formula weight	961.21	478.59	547.47
Temperature/K	150.01(10)	230.00(10)	150.00(10)
Crystal system	triclinic	monoclinic	monoclinic
Space group	P-1	P <sub>2</sub> <sub>1</sub> /c	P <sub>2</sub> <sub>1</sub> /n
a/Å	7.1811(2)	20.4315(15)	7.5544(7)
b/Å	14.9602(4)	12.3775(9)	25.0803(17)
c/Å	19.6044(6)	7.5999(6)	23.349(2)
α/°	102.583(2)	90	90
β/°	98.208(3)	92.791(7)	92.628(9)
γ/°	95.129(2)	90	90
Volume/Å <sup>3</sup>	2018.58(10)	1919.7(2)	4419.2(6)
Z	2	4	8
ρ <sub>calc</sub> /cm <sup>3</sup>	1.581	1.656	1.646
μ/mm <sup>-1</sup>	4.482	4.713	6.353
F(000)	984.0	976.0	2208.0
Crystal size/mm <sup>3</sup>	0.213 × 0.068 × 0.035	0.238 × 0.129 × 0.054	0.112 × 0.046 × 0.043
Radiation	CuKα (λ = 1.54184)	CuKα (λ = 1.54184)	CuKα (λ = 1.54184)
2θ range for data collection/°	6.1 to 144.37	8.354 to 151.948	5.174 to 144.28
Index ranges	-8 ≤ h ≤ 8, -18 ≤ k ≤ 18, -23 ≤ l ≤ 24	-25 ≤ h ≤ 24, -15 ≤ k ≤ 15, -9 ≤ l ≤ 9	-9 ≤ h ≤ 9, -29 ≤ k ≤ 30, -28 ≤ l ≤ 28
Reflections collected	14870	4844	23842
Independent reflections	7570 [R <sub>int</sub> = 0.0287, R <sub>sigma</sub> = 0.0403]	4844 [R <sub>int</sub> = 0.0345, R <sub>sigma</sub> = 0.0167]	7839 [R <sub>int</sub> = 0.1000, R <sub>sigma</sub> = 0.1164]
Data/restraints/parameters	7570/0/577	4844/0/290	7839/0/614
Goodness-of-fit on F <sup>2</sup>	1.018	1.085	1.043
Final R indexes [I >= 2σ (I)]	R <sub>1</sub> = 0.0343, wR <sub>2</sub> = 0.0828	R <sub>1</sub> = 0.0661, wR <sub>2</sub> = 0.2054	R <sub>1</sub> = 0.1021, wR <sub>2</sub> = 0.2570
Final R indexes [all data]	R <sub>1</sub> = 0.0431, wR <sub>2</sub> = 0.0873	R <sub>1</sub> = 0.0736, wR <sub>2</sub> = 0.2102	R <sub>1</sub> = 0.1566, wR <sub>2</sub> = 0.3033
Largest diff. peak/hole / e Å <sup>-3</sup>	0.33/-0.35	0.75/-0.63	0.89/-0.59

Figure S2. Structure of 2-bromonaphtho[2,1-b]-thiophene **2** with atom labels.

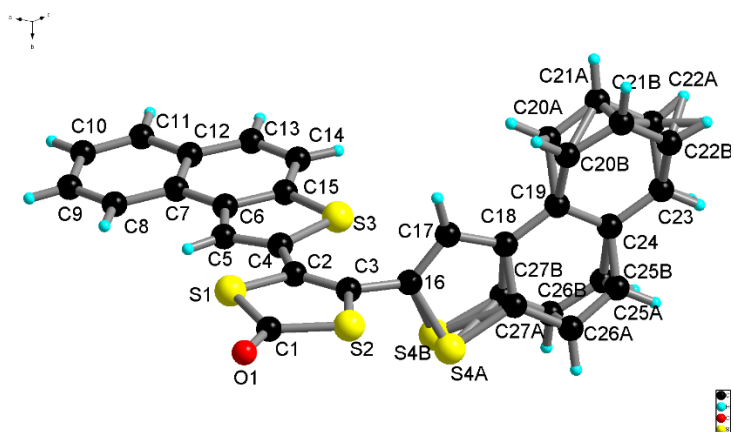


Figure S3. Structure of the bis-naphtho[2,1-b]-thiophene-1,3-dithiol-2-one **4** with atom labels.

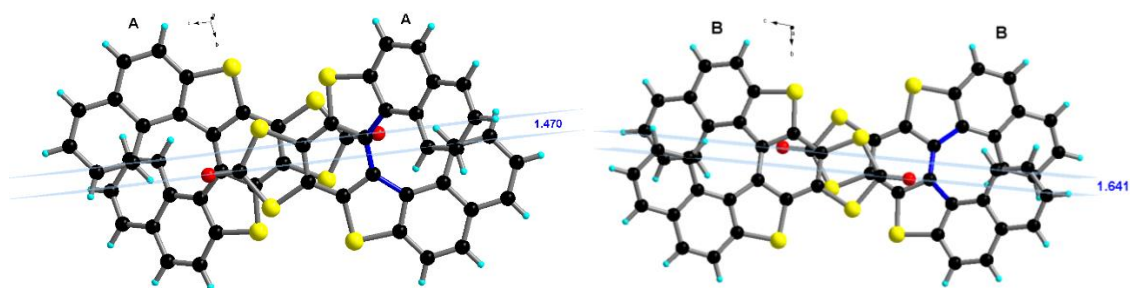
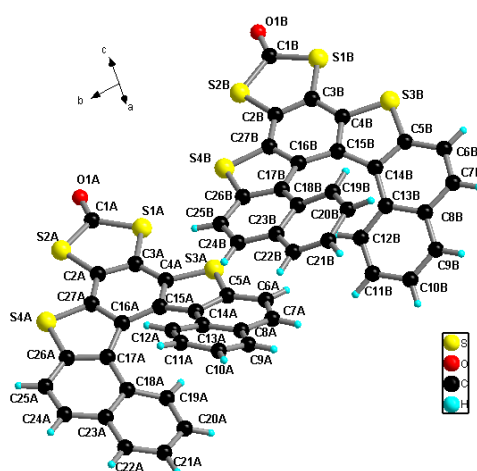


Figure S4. Structure of the of the dithia[7]helicene **1-dTH** with atom labels (top) and lateral shift (Å) of *head-to-tail* molecules **A** and **B** (bottom).

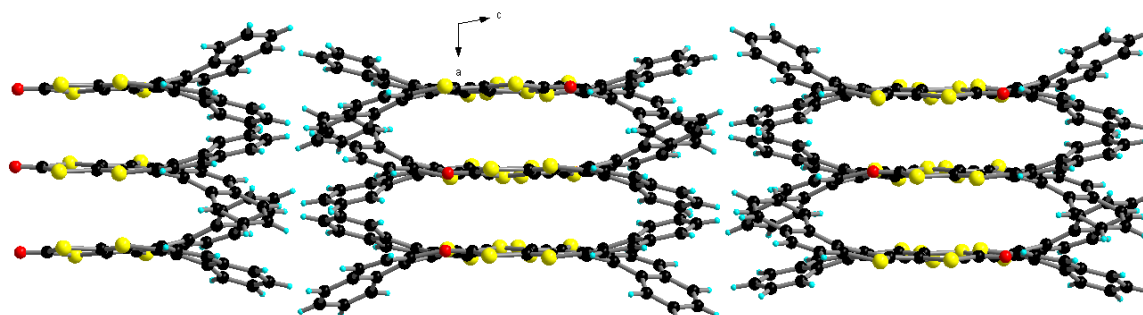


Figure S5. Packing of the dithia[7]helicene **1-dTH**, view along the *b* axis.

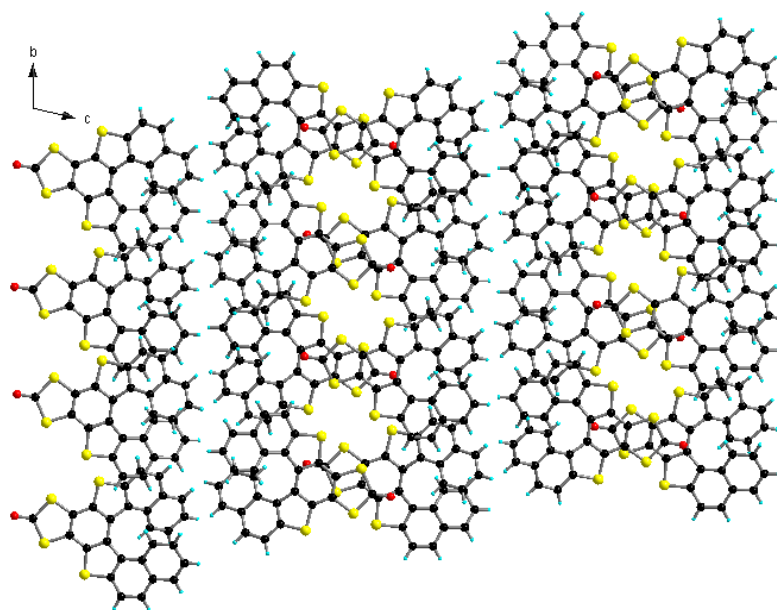


Figure S6. Packing of the dithia[7]helicene **1-dTH**, view along the *a* axis.

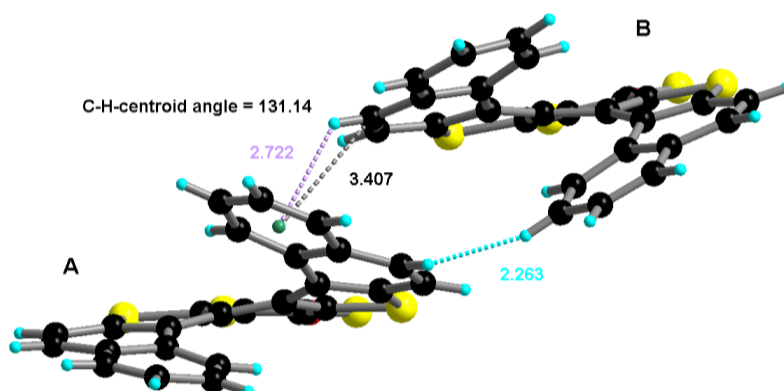


Figure S7. Intermolecular C-H $\cdots$  $\pi$  inter-stack interactions between molecules **A** and **B** of the dithia[7]helicene **1-dTH**.

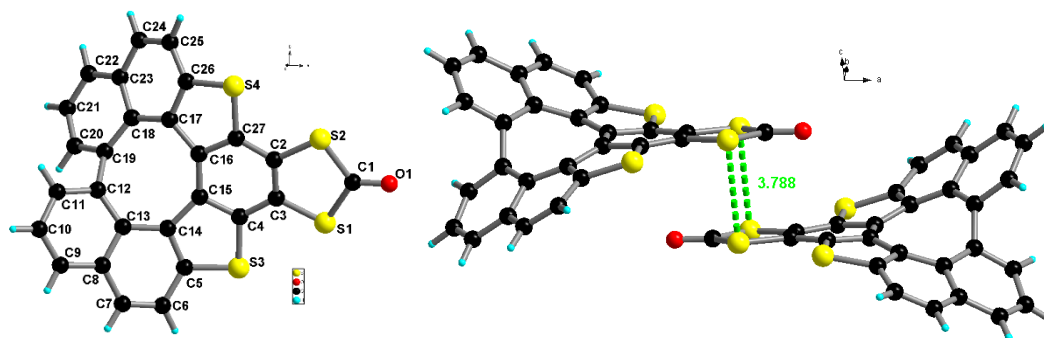


Figure S8. Structure of the quasi[8]circulene **1-dTQC** with atom labels and head to tail disposition together with  $S_{\text{dithiolene}}\cdots S_{\text{dithiolene}}$  (green) intra-stack distances ( $\text{\AA}$ ) between molecules.

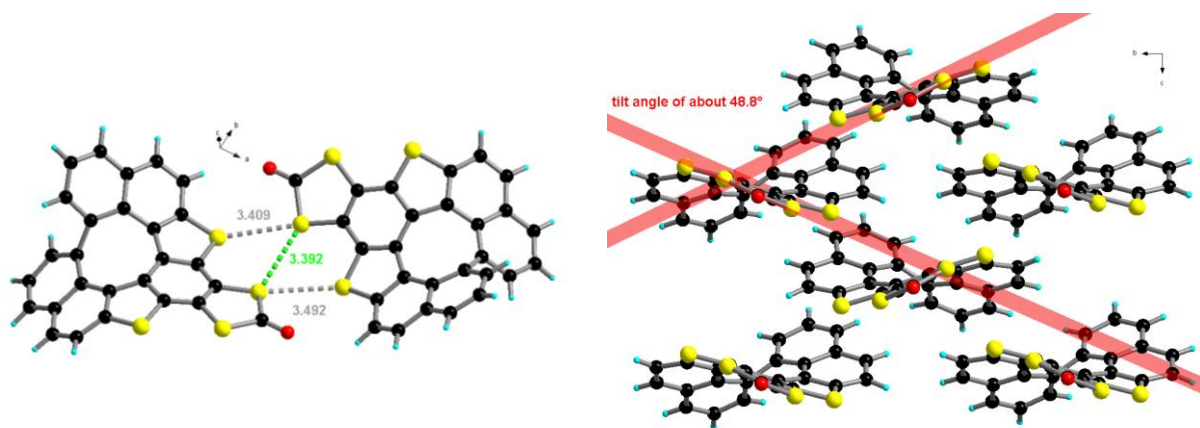


Figure S9. Tilt angle ( $^{\circ}$ ) and intermolecular lateral interactions ( $\text{\AA}$ ) between molecule of parallel layers together with  $S_{\text{th}} \cdots S_{\text{dithiolene}}$  (grey) and  $S_{\text{dithiolene}} \cdots S_{\text{dithiolene}}$  (green) in the structure of quasi[8]circulene **1-dTQC**.

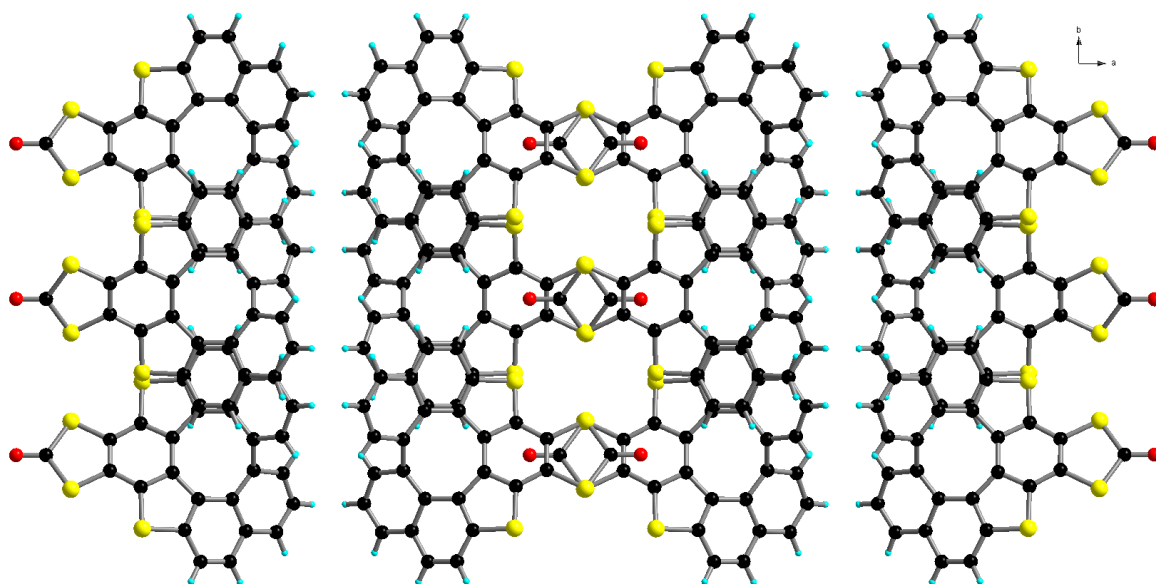


Figure S10. Packing of the quasi[8]circulene **1-dTQC**, view along the  $c$  axis.

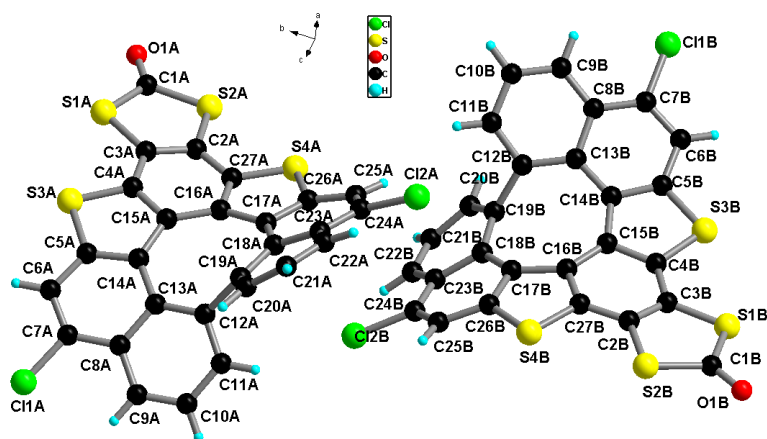


Figure S11. Structure of the quasi[8]circulene **1-dTQC-Cl** with atom labels.

Quasi[8]circulene **1-dTQC-Cl** crystallizes in the monoclinic system,  $P2_1/n$  space group, with two independent molecules in the unit cell (**A** and **B** of *M* and *P* helicity, respectively) similarly to **1-dTH**. The stacks along the *a* axis are formed by alternate **A** and **B** type molecules which rotate with respect to each other of about  $85^\circ$  and interact through  $S_{th} \cdots S_{dithiolene}$  (grey) and  $S_{dithiolene} \cdots S_{dithiolene}$  (green) contacts. The stacks of molecules interact in a *head-to-tail* fashion along *c* through  $O \cdots Cl$  contacts and laterally along *b* through  $C-Cl \cdots \pi$  contacts (Figures S12 - S14).

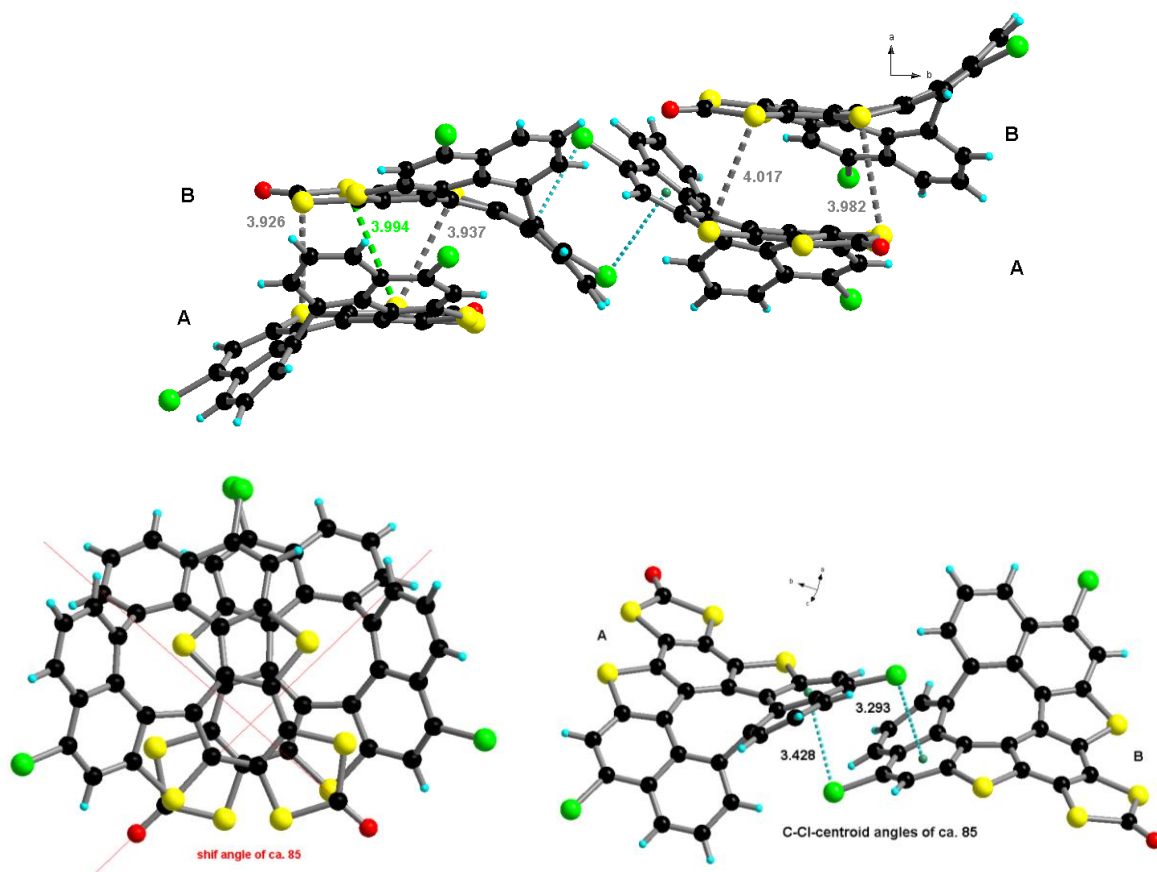


Figure S12. View of the intermolecular interactions ( $\text{\AA}$ ) between molecules of type **A** and molecules of type **B**,  $S_{th} \cdots S_{dithiolene}$  (grey),  $S_{dithiolene} \cdots S_{dithiolene}$  (green) and  $C-Cl \cdots \pi$  (distance between the Cl atom and the centroid of the phenyl ring) in the *ab* plane (top) and shift of molecules in the stack (left) and  $C-Cl \cdots \pi$  interactions (right) in the quasi[8]circulene **1-dTQC-Cl** (bottom).



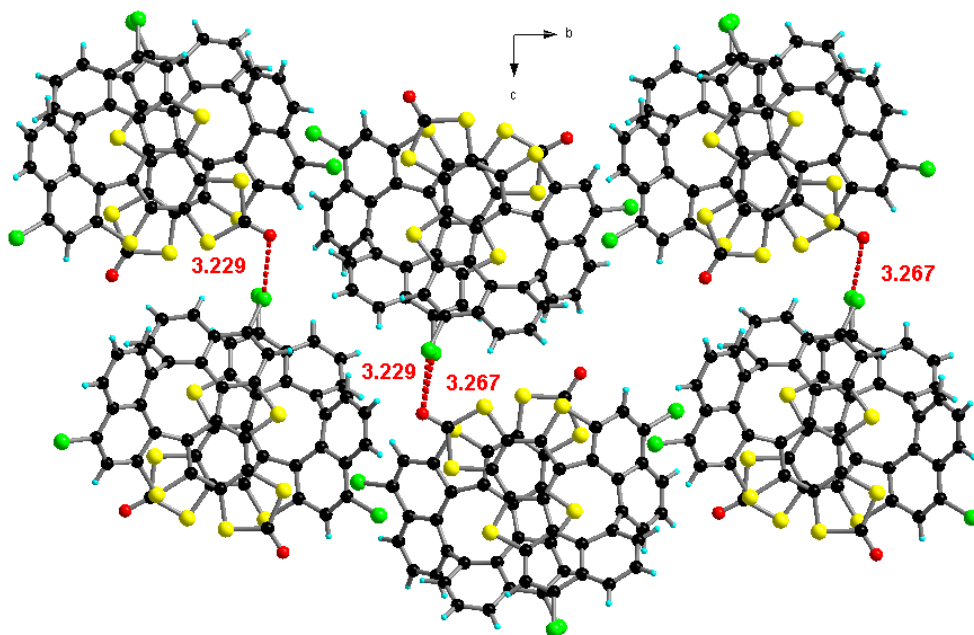


Figure S13. Packing within quasi[8]circulene **1-dTQC-Cl**, view in the *bc* plane and a highlight of the O $\cdots$ Cl interactions (red).

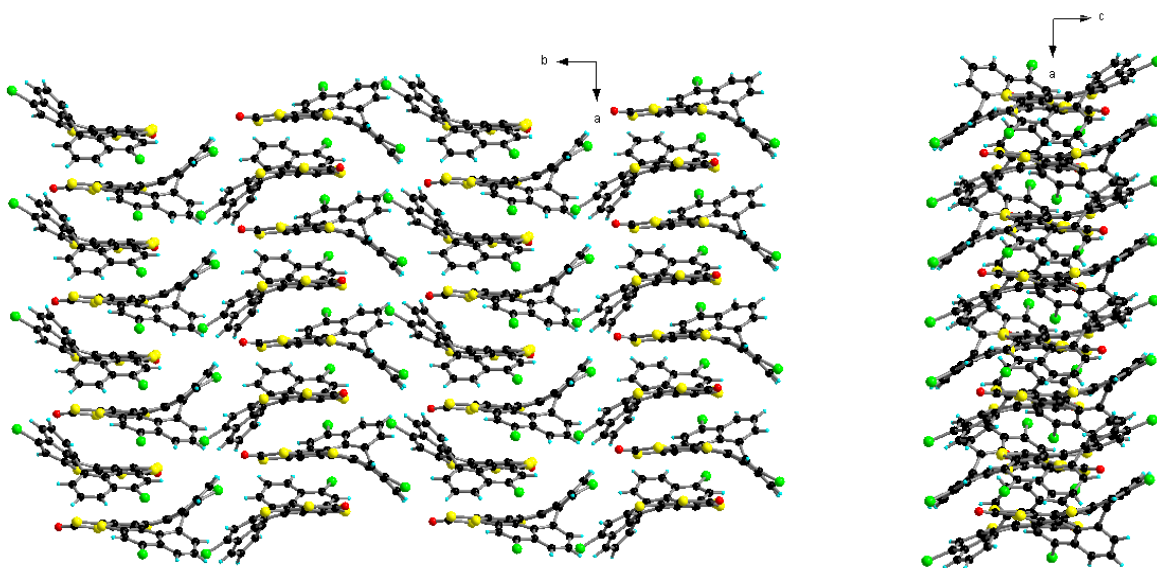


Figure S14. Packing of the quasi[8]circulene **1-dTQC-Cl**, in the *ab* plane (left) and *ac* plane (right).

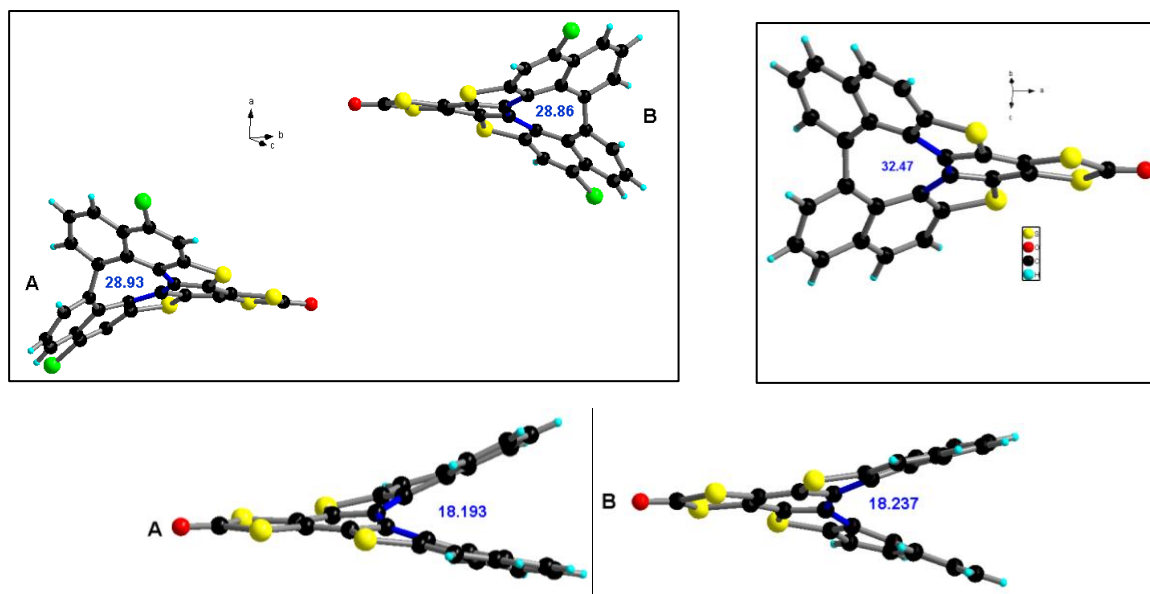


Figure S15. The helicenic torsion seen through the dihedral angles ( $^{\circ}$ ) in the centre of the helix in quasi[8]circulene **1-dTQC-Cl** (top, left), quasi[8]circulene **1-dTQC** (top, right) and dithia[7]helicene **1-dTH** (bottom).

#### 4. Racemisation barrier and enantiomer resolution

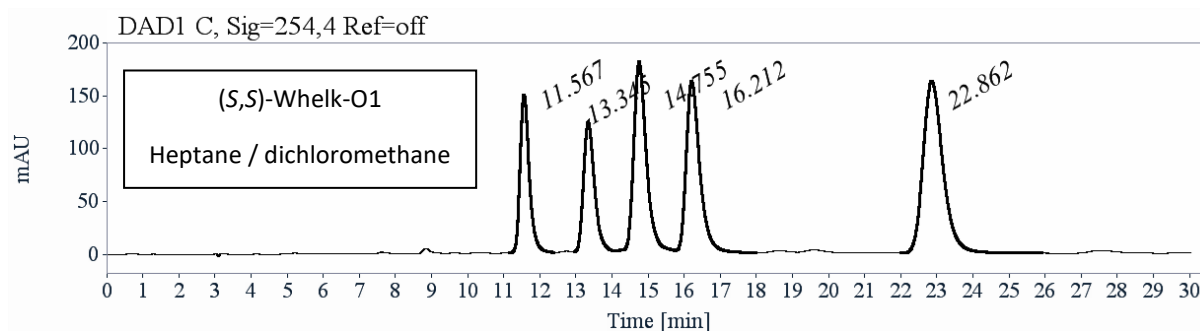
Table S4. Estimated and experimentally determined racemisation energies of known dihetero[7]helicene.

Racemisation energy DFT (exp) (kcal/mol)	[7]Helicenes		Ref.
	1	<b>dTH(S)</b>	
2	<b>dOH(O)</b>	22.5 (22.2)	
3	<b>dOAH(ON)</b>	24.8	
4	<b>dAH(N)</b>	26.5	
5	<b>dAH-OMe(N)</b>	- (31.7)	
6	<b>dAH(NTs)</b>	34.9	
7	<b>dAH(NtBu)</b>	27.4	

##### 4.1. Chiral HPLC

Analytical chiral HPLC separation for mixture of **1-dTH** (*rac*), **1-dTQC** (*rac*) compounds and unreacted precursor **4** (the fifth peak at 22.862 retention time).

• The sample is dissolved in dichloromethane, injected on the chiral column, and detected with an UV detector at 254 nm and a circular dichroism detector at 254 nm. The flow-rate is 1 mL/min.



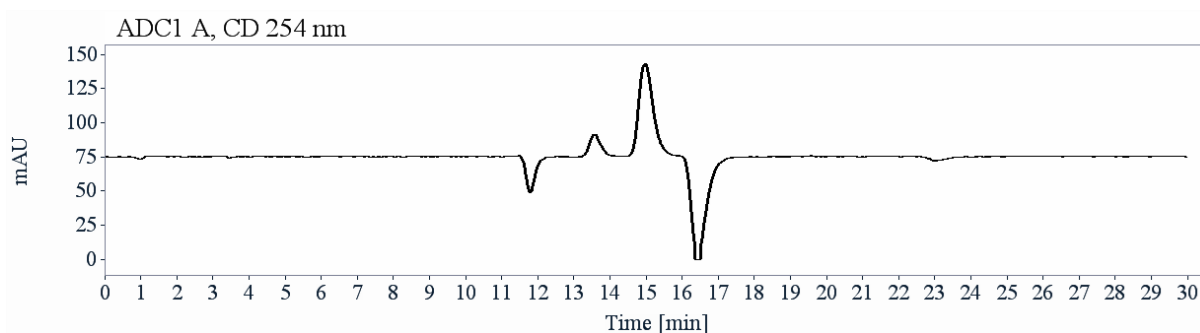


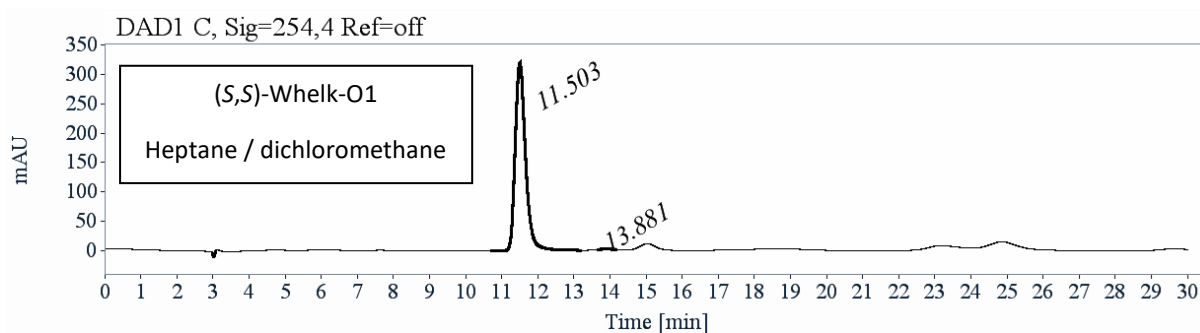
Figure S16. Analytical chiral HPLC separation for a mixture of **1-dTH** (*rac*) and **1-dTQC** (*rac*).

RT [min]	Area	Area%	Capacity Factor
11.57	2661	13.13	2.92
13.34	2622	12.93	3.52
14.75	4463	22.02	4.00
16.21	4257	21.00	4.50
22.86	6267	30.92	6.75
Sum	20270	100.00	

Semi-preparative separation for a mixture of **1-dTH** (*rac*) and **1-dTQC** (*rac*):

**The first separation aims to collect the first peak and the last peak.**

- Sample preparation: About 89 mg of mixture are dissolved in 84 mL of dichloromethane.
- Chromatographic conditions: (*S,S*)-Whelk-O1 (250 x 10 mm), hexane / dichloromethane (50/50) as mobile phase, flow-rate = 5 mL/min, UV detection at 254 nm.
- Injections (stacked): 280 times 300  $\mu$ L, every 4 minutes.
- Chromatograms of the collected fractions:
- First fraction: 12 mg of **1-dTH** (*M*), with ee > 98%, first eluted peak

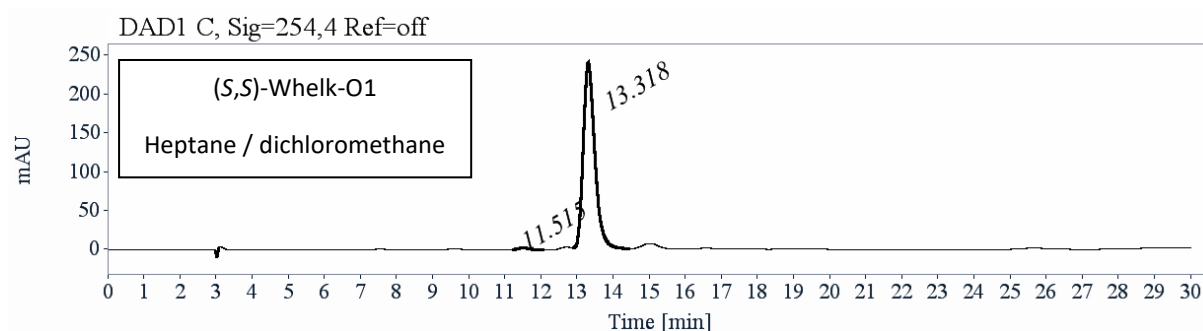


RT [min]	Area	Area%
11.50	6444	99.24
13.88	49	0.76
Sum	6493	100.00

- Second fraction: 35 mg of the second, third and fourth peaks.

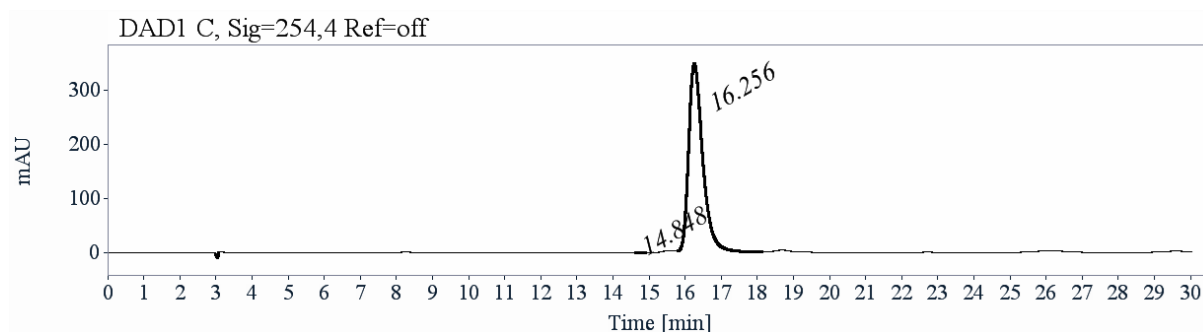
**The second separation aims to collect the three other compounds.**

- Sample preparation: About 35 mg of mixture are dissolved in 112 mL of dichloromethane.
- Chromatographic conditions: Chiralpak IE (250 x 10 mm), hexane / dichloromethane (50/50) as mobile phase, flow-rate = 5 mL/min, UV detection at 254 nm.
- Injections (stacked): 140 times 800  $\mu$ L, every 8 minutes.
- First fraction: 7 mg of **1-dTH** (*P*), with ee > 98%, first eluted peak



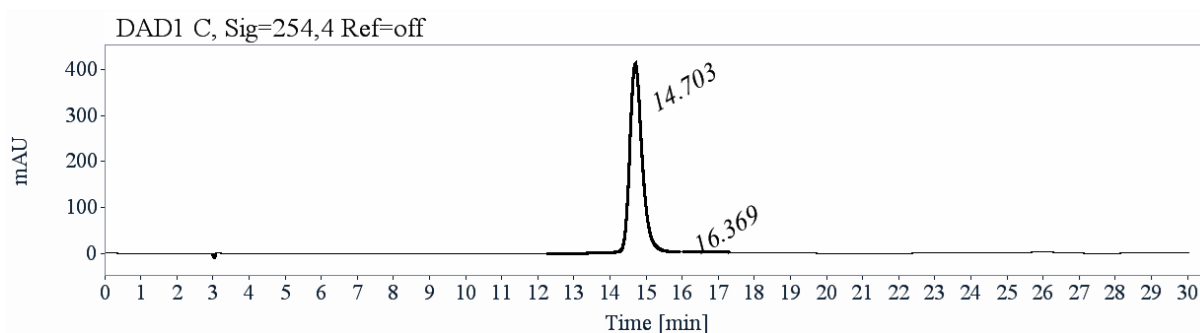
RT [min]	Area	Area%
11.51	49	0.89
13.32	5423	99.11
Sum	5471	100.00

- Second fraction: 10 mg of **1-dQC** (*P*), with ee > 99%, first eluted peak



RT [min]	Area	Area%
14.85	8	0.08
16.26	9587	99.92
Sum	9595	100.00

- Third fraction: 10 mg of **1-dQC** (*M*), with ee > 98%, first eluted peak



RT [min]	Area	Area%
14.70	10132	99.47
16.37	54	0.53
Sum	10186	100.00

#### 4.2. Optical rotations

Optical rotations were measured on a Jasco P-2000 polarimeter with a sodium lamp (589 nm), a halogen lamp (578 and 546 nm), in a 10 cm cell, thermostated at 25°C with a Peltier controlled cell holder.

Table S5. Optical rotations for **1-dTH**.

$\lambda$ (nm)	<b>1-dTH (M)</b>	<b>1-dTH (P)</b>
	First eluted enantiomer on (S,S)-Whelk-O1 $[\alpha]_{\lambda}^{25}$ (CH <sub>2</sub> Cl <sub>2</sub> , c=0.10)	Second eluted enantiomer on (S,S)-Whelk-O1 $[\alpha]_{\lambda}^{25}$ (CH <sub>2</sub> Cl <sub>2</sub> , c=0.10)
589	- 1050	+ 1050
578	- 1100	+ 1100
546	- 1300	+ 1300

Table S6. Optical rotations for **1-dTQC**.

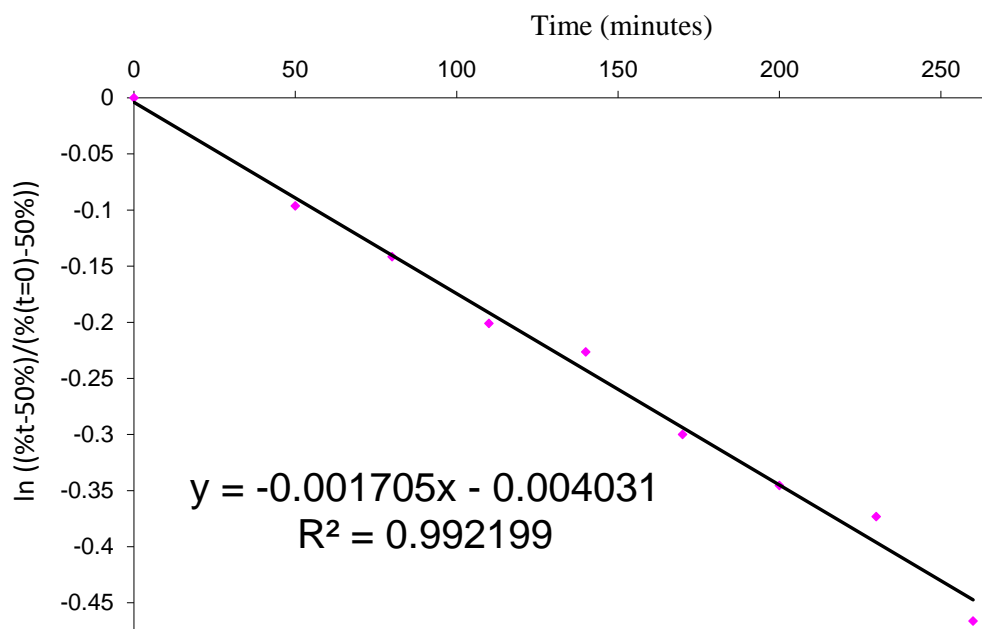
$\lambda$ (nm)	<b>1-dTQC (M)</b>	<b>1-dTQC (P)</b>
	Third eluted enantiomer on (S,S)-Whelk-O1 $[\alpha]_{\lambda}^{25}$ (CH <sub>2</sub> Cl <sub>2</sub> , c=0.08)	Fourth eluted enantiomer on (S,S)-Whelk-O1 $[\alpha]_{\lambda}^{25}$ (CH <sub>2</sub> Cl <sub>2</sub> , c=0.09)
589	- 700	+ 700
578	- 750	+ 750
546	- 1000	+ 1000

### 4.3. Kinetic of enantiomerisation

#### 1-dTH in 1,2-dichlorobenzene

About 0.5 mg of (*M*)-1-dTH is heated in about 15 mL of 1,2-dichlorobenzene at 180 °C. 20 µL are taken and then injected on Chiralpak ID (70:30 heptane / dichloromethane, 1 mL/min, UV 310 nm,  $R_t(P) = 6.17$  min,  $R_t(M) = 7.29$  min,  $k(P) = 1.09$ ,  $k(M) = 1.47$ ,  $\alpha = 1.35$  and  $R_s = 3.49$ ). The percentage decrease of (*M*)-1-dTH is monitored.

Time (min)	% ( <i>M</i> )-1-dTH	$\ln ((\%t-50\%)/(\%t=0)-50\%))$
0	97.999	0.00000
50	93.59	-0.09635
80	91.661	-0.14161
110	89.262	-0.20092
140	88.277	-0.22633
170	85.557	-0.30004
200	83.979	-0.34544
230	83.051	-0.37313
260	80.112	-0.46626



$k_{\text{enantiomerisation}} = 1.42 \cdot 10^{-5} \text{ s}^{-1}$  (180 °C, 1,2-dichlorobenzene)

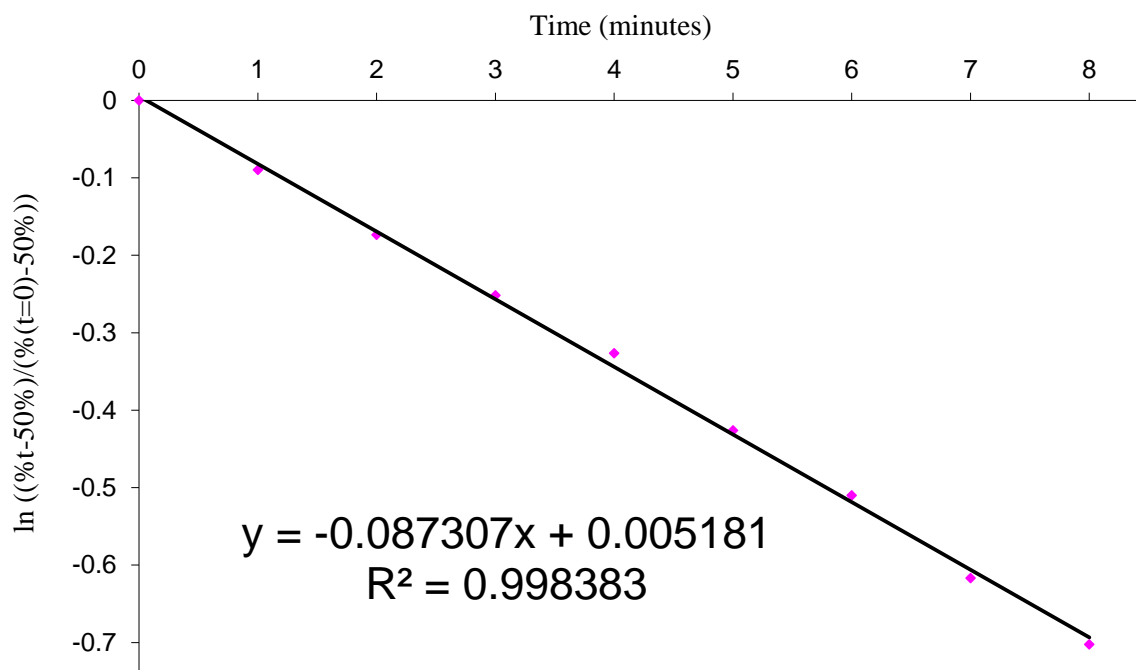
$\Delta G^\ddagger = 154.6 \text{ kJ} \cdot \text{mol}^{-1} = 37.0 \text{ kcal} \cdot \text{mol}^{-1}$  (180 °C, 1,2-dichlorobenzene)

$t_{1/2} = 6.8$  hours (180 °C, 1,2-dichlorobenzene)

### 1-dTQC in chlorobenzene

About 0.5 mg of the second eluted enantiomer of (*M*)-1-dTQC is heated in about 15 mL of chlorobenzene at 132 °C. 20  $\mu$ L are taken and then injected on Chiralpak IF (70:30 heptane / dichloromethane, 1 mL/min, UV 310 nm,  $R_t(P)$  = 10.36 min,  $R_t(M)$  = 12.19 min,  $k(P)$  = 2.51,  $k(M)$  = 3.13,  $\alpha$  = 1.25 and  $R_s$  = 3.66). The percentage decrease of the second eluted enantiomer of (*M*)-1-dTQC is monitored.

Time (min)	% ( <i>M</i> )-1-dTQC	$\ln ((\%t-50\%)/(\%t=0)-50\%))$
0	96.087	0.00000
1	92.131	-0.08975
2	88.75	-0.17340
3	85.836	-0.25158
4	83.255	-0.32633
5	80.096	-0.42614
6	77.672	-0.51011
7	74.872	-0.61679
8	72.833	-0.70232



$k_{\text{enantiomerisation}} = 7.28 \cdot 10^{-4} \text{ s}^{-1}$  (132 °C, chlorobenzene)

$\Delta G^\ddagger = 124.6 \text{ kJ} \cdot \text{mol}^{-1} = 29.8 \text{ kcal} \cdot \text{mol}^{-1}$  (132 °C, chlorobenzene)

$t_{1/2} = 8 \text{ minutes}$  (132 °C, chlorobenzene)

## 5. Absorption and circular dichroism properties

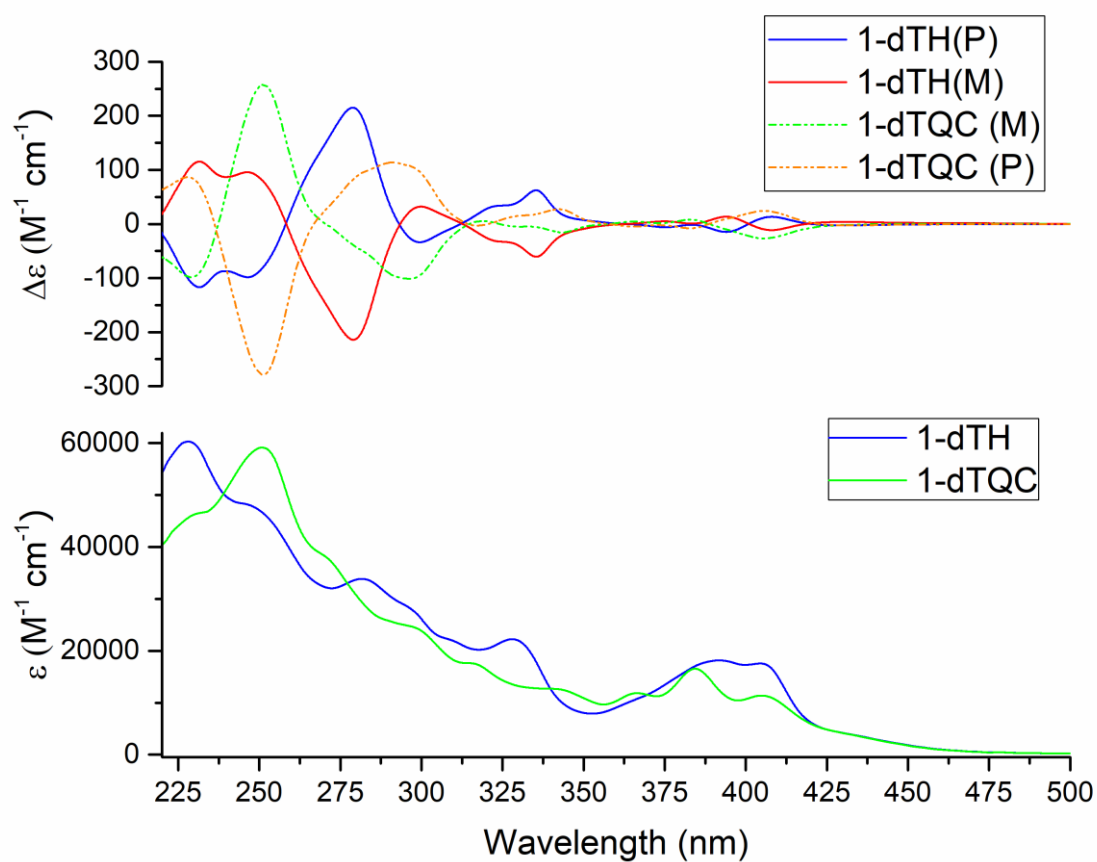


Figure S17. CD spectra (top) of **1-dTH** and **1-dTQC** 0.19 mM in dichloromethane, together with their absorption spectra (bottom).



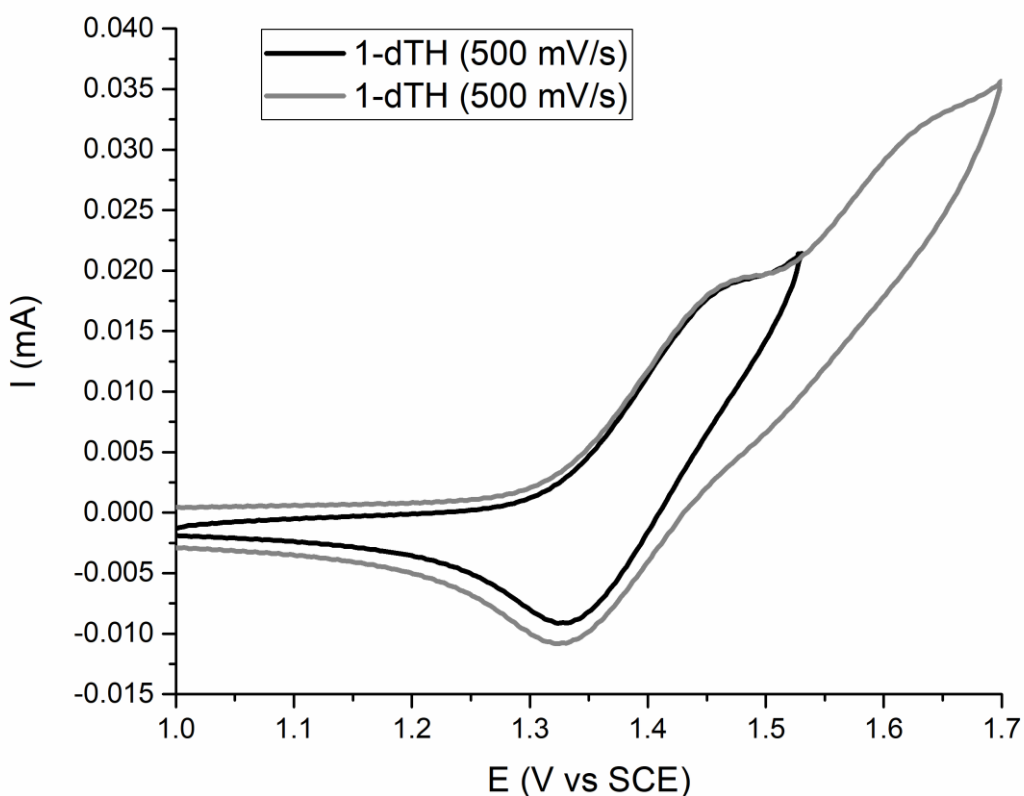


Figure S18. Cyclic voltammetry of **1-dTH** (1.24 mM) using TBAPF<sub>6</sub> electrolyte (100 mM solution in dichloromethane) at 500 mN/s up to 1.5 and 1.7 V.

## 6. Theoretical calculations

### 6.1. Computational details

All calculations were performed with the Gaussian 09 program version D01.<sup>4</sup> Based on the good results obtained in previous studies on helicenes,<sup>5</sup> we have chosen to use again a DFT method with the hybrid functional PBE0 (with 25% of exact exchange).<sup>6</sup> The 6-311+G(2d,p) Pople type augmented basis set has been chosen. Ground states and transition states geometries were optimized with default parameters. Transition states were built and optimized thanks to symmetry restrictions (flat or saddle forms). We have then verified by a frequency calculation that the converged geometries correspond to global minimum or transition states (with only one negative frequency) on the potential energy surface. The gas phase excited states energies have been determined at the same level of theory by a linear response Time-Dependent DFT method considering the first singlet-to-singlet excitations. Molecular orbitals (MO), density difference plots (between ground and excited state) pictures have been generated by quchemreport,<sup>7</sup> a homemade automated quality control and report generation python program based on cclib.<sup>8</sup> The calculated bar spectra have been enlarged with a Gaussian shape (FWHM=3000cm<sup>-1</sup>) with quchemreport to compare with the experiment.

## 6.2. Results

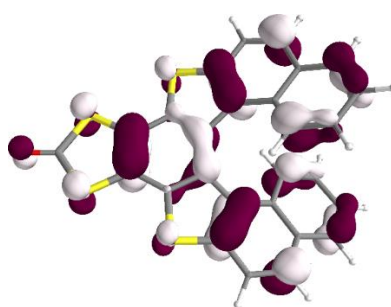


Figure S19. SOMO topology of **1-dTH-cat**.

Table S7. Representation of the frontier orbitals of **1-dTH (M)** and **1-dTQC (M)** together with the corresponding orbital energy values (eV).

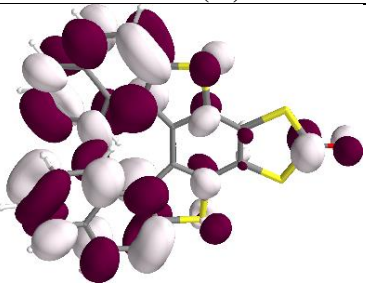
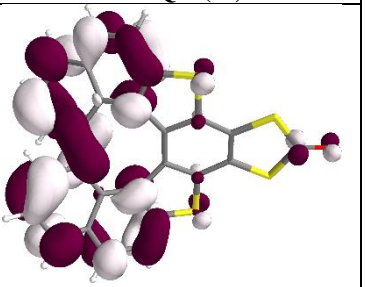
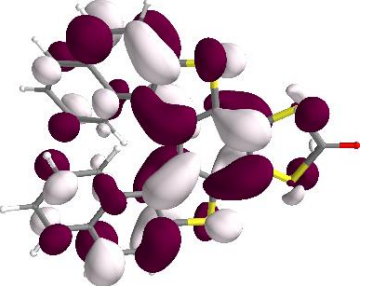
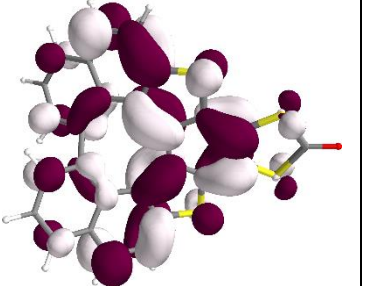
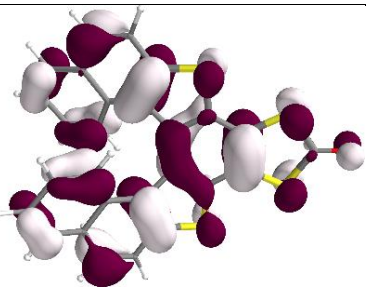
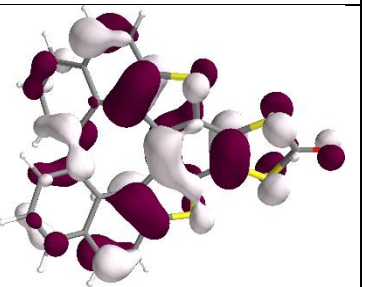
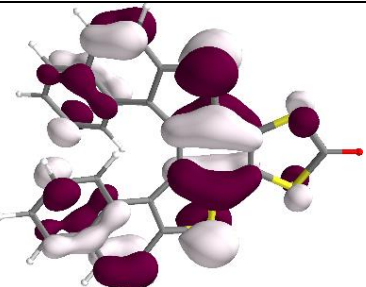
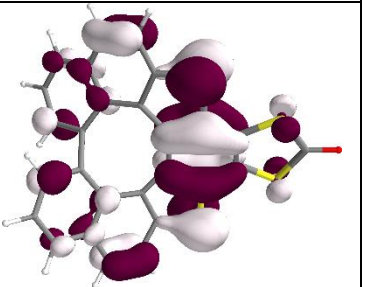
	<b>1-dTH (M)</b>	<b>1-dTQC (M)</b>
<b>LUMO+1</b>	 -1.46 eV	 -1.64 eV
<b>LUMO</b>	 -2.22 eV	 -2.13 eV
<b>HOMO</b>	 -5.98 eV	 -5.99 eV
<b>HOMO-1</b>	 -6.29 eV	 -6.31 eV

Table S8. The calculated mono-electronic excitations and the density difference between the fundamental and the excited states for the highlighted transitions (excited electron in green and hole in white) for the **1-dTH** (*M*).

Table. Results concerning the calculated mono-electronic excitations									
E.S.	Symmetry	nm	cm-1	f	R	Lambda	dCT	qCT	Excitation description in %
1	Singlet-A	399	25046	0.173	-77.1881	0.78	18.81	0.41	123->124 (96)
2	Singlet-A	370	26960	0.129	80.395	0.73	18.82	0.45	121->124 (2) 122->124 (87) 123->127 (4) 123->128 (2)
3	Singlet-A	332	30100	0.019	11.7865	0.71	189.55	0.46	121->124 (79) 123->125 (16)
4	Singlet-A	330	30275	0.010	-15.6466	0.46	420.24	0.73	119->126 (4) 123->126 (89)
5	Singlet-A	320	31187	0.117	-41.5839	0.75	181.00	0.35	121->124 (14) 123->125 (80)
6	Singlet-A	314	31837	0.023	-165.9448	0.61	13.52	0.37	119->124 (12) 120->124 (40) 122->125 (30) 123->129 (8)
7	Singlet-A	306	32660	0.000	0.2599	0.46	387.35	0.68	122->126 (86) 123->127 (4) 123->128 (2)
8	Singlet-A	299	33443	0.005	5.2	0.64	19.55	0.45	119->124 (11) 120->124 (47) 122->125 (37)
9	Singlet-A	296	33680	0.004	-14.1771	0.59	105.74	0.46	119->124 (70) 122->125 (23)
10	Singlet-A	294	33988	0.167	138.732	0.63	366.80	0.50	118->124 (5) 122->124 (3) 122->126 (2) 123->127 (78) 123->131 (4)
11	Singlet-A	287	34768	0.112	107.3398	0.62	348.22	0.32	118->124 (11) 119->125 (2) 120->125 (10) 122->124 (2) 122->126 (4) 122->130 (2) 123->127 (3) 123->128 (44) 123->131 (8)
12	Singlet-A	280	35708	0.007	16.3292	0.64	321.33	0.33	118->124 (27) 123->127 (4) 123->128 (38) 123->131 (21)
13	Singlet-A	278	35879	0.032	-106.5614	0.65	113.57	0.35	121->125 (18) 122->127 (44) 123->129 (17) 123->130 (15)
14	Singlet-A	278	35969	0.007	-18.3107	0.64	193.70	0.30	120->124 (2) 121->125 (39) 122->125 (4) 123->129 (35) 123->130 (5)
15	Singlet-A	273	36505	0.071	-412.5608	0.65	112.66	0.39	120->124 (2) 121->127 (3) 122->127 (9) 122->128 (8) 123->129 (7) 123->130 (62)
16	Singlet-A	271	36782	0.059	1.6039	0.61	241.31	0.37	121->125 (21) 122->127 (33) 122->128 (26) 123->129 (9)
17	Singlet-A	269	37116	0.010	17.8532	0.42	517.38	0.60	118->124 (12) 121->126 (66) 122->130 (2) 123->131 (3) 123->132 (5)
18	Singlet-A	264	37745	0.088	-42.4283	0.58	253.40	0.37	120->126 (4) 121->125 (14) 121->127 (2) 122->128 (51) 122->132 (3) 123->129 (4) 123->130 (6)
19	Singlet-A	263	37914	0.013	-12.8598	0.61	179.49	0.27	118->124 (27) 120->125 (5) 121->126 (15) 122->129 (17) 122->130 (9) 123->131 (17)
20	Singlet-A	257	38857	0.009	-88.2624	0.50	483.61	0.57	120->126 (2) 121->127 (58) 121->128 (20) 122->128 (2) 122->131 (2) 123->130 (3)

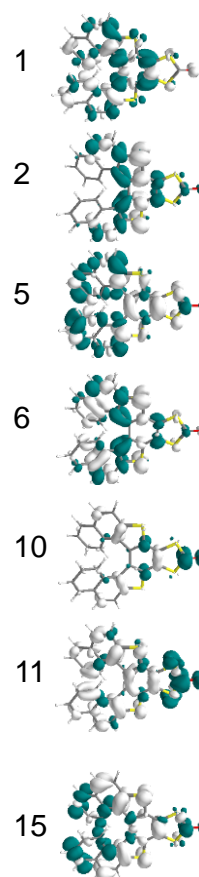
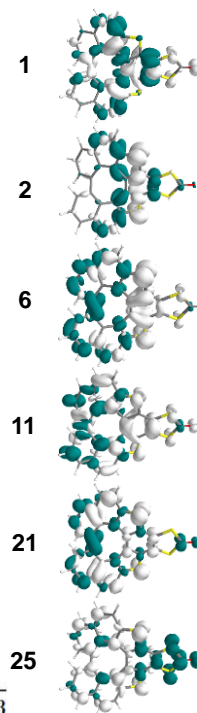


Table S9. The calculated mono-electronic excitations and the density difference between the fundamental and the excited states for the highlighted transitions (excited electron in green and hole in white) for the **1-dTQC** (*M*).

Table. First five calculated mono-electronic excitations and those with  $f > 0.1$  or  $R > 10$ .

E.S.	Symmetry	nm	cm <sup>-1</sup>	$f$	R	$\Lambda$	$d_{CT}$	$q_{CT}$	Excitation description : initial OM - ending OM (% if > 5%)
1	Singlet-A	394	25375	0.131	-119.4	0.78	113.33	0.40	122-123(96);
2	Singlet-A	357	27983	0.118	112.4	0.74	63.74	0.40	120-123(11); 121-123(74);
3	Singlet-A	345	28943	0.023	29.3	0.70	108.47	0.33	120-123(42); 121-123(13); 122-124(40);
4	Singlet-A	339	29460	0.000	0.7	0.43	383.42	0.77	122-125(93);
5	Singlet-A	334	29915	0.062	9.4	0.68	196.09	0.34	120-123(39); 122-124(53);
6	Singlet-A	322	31012	0.010	-138.8	0.60	319.15	0.36	119-123(24); 120-124(11); 121-124(40); 122-127(16);
8	Singlet-A	307	32497	0.000	-13.9	0.66	155.81	0.35	119-123(42); 120-124(16); 121-124(27); 122-127(12);
9	Singlet-A	303	32897	0.099	59.7	0.68	193.19	0.45	120-124(65); 121-124(27);
10	Singlet-A	301	33199	0.092	25.6	0.55	447.78	0.56	122-126(77);
11	Singlet-A	294	33959	0.051	-326.7	0.59	271.73	0.34	119-123(26); 122-127(59);
12	Singlet-A	289	34566	0.031	16.1	0.58	168.53	0.29	119-124(31); 120-125(9); 120-127(6); 121-127(8); 122-126(11); 122-128(6); 122-129(11);
14	Singlet-A	279	35841	0.017	-21.5	0.61	181.07	0.34	118-123(47); 121-126(39);
15	Singlet-A	277	35977	0.011	20.9	0.65	148.96	0.42	117-123(7); 122-128(58); 122-129(13);
17	Singlet-A	272	36754	0.011	-18.7	0.61	353.19	0.52	119-124(14); 120-127(7); 121-127(71);
18	Singlet-A	269	37090	0.039	15.7	0.69	45.87	0.40	120-127(32); 121-127(7); 122-128(9); 122-129(39);
19	Singlet-A	265	37637	0.051	-17.3	0.52	424.16	0.41	120-126(36); 122-130(37);
21	Singlet-A	262	38120	0.283	66.5	0.66	44.29	0.31	117-123(57); 119-124(6); 120-127(9); 122-128(7); 122-129(8);
23	Singlet-A	257	38781	0.051	-45.9	0.64	116.51	0.35	117-124(8); 120-128(6); 121-128(44); 121-129(16);
24	Singlet-A	254	39295	0.086	-89.2	0.58	324.77	0.42	120-128(29); 120-129(21); 121-128(18); 122-130(12);
25	Singlet-A	252	39589	0.150	195.2	0.63	363.16	0.31	117-123(9); 118-124(28); 119-124(18); 120-127(10); 121-130(17);



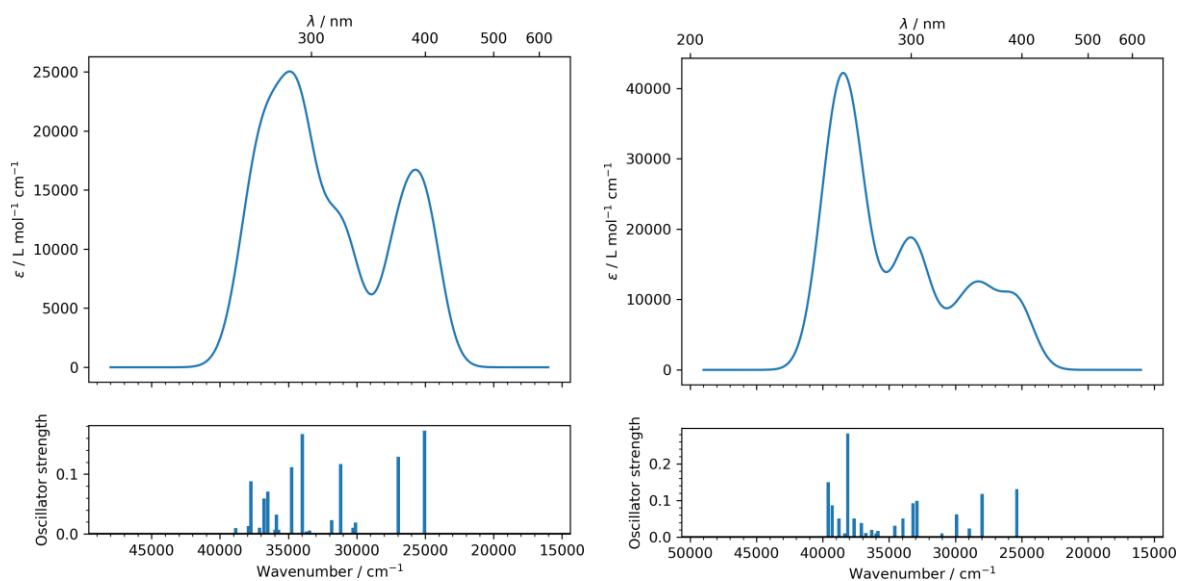


Figure S20. Calculated UV visible Absorption spectrum with a gaussian broadening (FWHM = 3000  $\text{cm}^{-1}$ ) for the **1-dTH (M)** (left) and **1-dTQC (M)** (right).

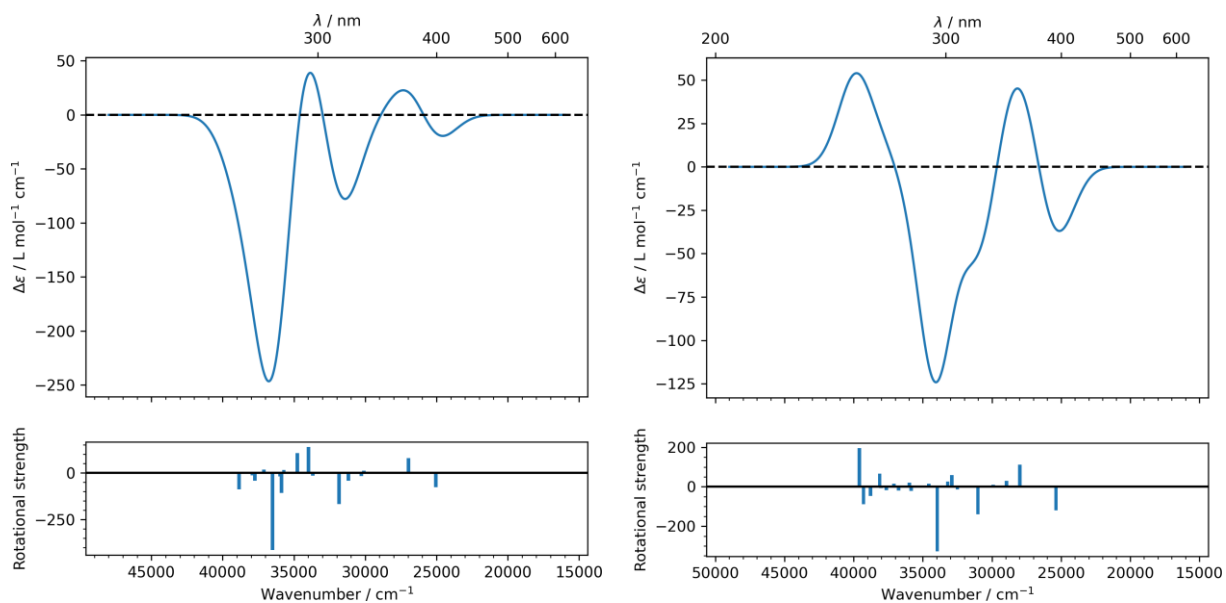


Figure S21. Calculated Circular Dichroism spectrum with a gaussian broadening (FWHM = 3000  $\text{cm}^{-1}$ ) for the **1-dTH (M)** (left) and **1-dTQC (M)** (right).

- 
- <sup>1</sup> B. Rungtaweeworanit, A. Butsuri, K. Wongma, K. Sadorn, K. Neranon, C. Nerungsi and T. Thongpanchang, *Tetrahedron Lett.* **2012**, *53*, 1816–1818.
- <sup>2</sup> a) K. Krajewski, Y. Zhang, D. Parrish, J. Deschamps, P. P. Rollera, V. K. Pathak *Bioorg. Med. Chem. Lett.* **2006**, *16*, 3034–3038; b) K. Clarke, G. Rawson and R. M. Scrowston, *J. Chem. Soc. C* **1969**, *4*, 537–540.
- <sup>3</sup> a) R. Irie, A. Tanoue, S. Urakawa, T. Imahori, K. Igawa, T. Matsumoto, K. Tomooka, S. Kikuta, T. Uchida and T. Katsuki *Chem. Lett.* **2011**, *40*, 1343–1345; b) Y. Kitahara and K. Tanaka, *Chem. Commun.* **2002**, 932–933; c) M. B. Groen, H. Schadenberg and H. Wynberg *J. Org. Chem.* **1971**, *36*, 2797–2809; d) M. B. Groen and H. Wynberg *J. Am. Chem. Soc.* **1971**, *93*, 2968–2974; e) S. Arae, T. Mori, T. Kawatsu, D. Ueda, Y. Shigeta, N. Hamamoto, H. Fujimoto, M. Sumimoto, T. Imahori, K. Igawa, K. Tomooka, T. Punniyamurthy, and R. Irie *Chem. Lett.* **2017**, *46*, 1214–1216.
- <sup>4</sup> M. J. Frisch, G. W. Trucks, H. B. Schlegel, G. E. Scuseria, M. A. Robb, J. R. Cheeseman, G. Scalmani, V. Barone, B. Mennucci, G. A. Petersson, H. Nakatsuji, M. Caricato, X. Li, H. P. Hratchian, A. F. Izmaylov, J. Bloino, G. Zheng, J. L. Sonnenberg, M. Hada, M. Ehara, K. Toyota, R. Fukuda, J. Hasegawa, M. Ishida, T. Nakajima, Y. Honda, O. Kitao, H. Nakai, T. Vreven, J. A. Montgomery Jr., J. E. Peralta, F. Ogliaro, M. Bearpark, J. J. Heyd, E. Brothers, K. N. Kudin, V. N. Staroverov, R. Kobayashi, J. Normand, K. Raghavachari, A. Rendell, J. C. Burant, S. S. Iyengar, J. Tomasi, M. Cossi, N. Rega, J. M. Millam, M. Klene, J. E. Knox, J. B. Cross, V. Bakken, C. Adamo, J. Jaramillo, R. Gomperts, R. E. Stratmann, O. Yazyev, A. J. Austin, R. Cammi, C. Pomelli, J. W. Ochterski, R. L. Martin, K. Morokuma, V. G. Zakrzewski, G. A. Voth, P. Salvador, J. J. Dannenberg, S. Dapprich, A. D. Daniels, Ö. Farkas, J. B. Foresman, J. V. Ortiz, J. Cioslowski and D. J. Fox, *Gaussian ~09 Revision D.01*, .
- <sup>5</sup> K. Martin, C. Melan, T. Cauchy and N. Avarvari, *ChemPhotoChem*, DOI:[10.1002/cptc.202100215](https://doi.org/10.1002/cptc.202100215).
- <sup>6</sup> a) J. P. Perdew, K. Burke and M. Ernzerhof, *Physical review letters*, 1996, **77**, 3865–3868; b) C. Adamo and V. Barone, *The Journal of Chemical Physics*, 1999, **110**, 6158–6170.
- <sup>7</sup> T. Cauchy and B. Da Mota, *quchemreport. A python program for control quality and automatic generation of quantum chemistry results*, University of Angers, **2020**.
- <sup>8</sup> N. M. O’boyle, A. L. Tenderholt, K. M. Langner, *J. Comput. Chem.* **2008**, *29*, 839–845.